Phospholipases Dζ1 and Dζ2 have distinct roles in growth and antioxidant systems in Arabidopsis thaliana responding to salt stress

Alhem Ben Othman, Hasna Ellouzi, Séverine Planchais, Delphine de Vos, Bualuang Faiyue, Pierre Carol, Chedly Abdelly, Arnould Savouré

Phopholipases Dζ1 and Dζ2 have distinct roles in growth and antioxidant systems in *Arabidopsis thaliana* responding to salt stress

Ahlem Ben Othman[1,2], Hasna Ellouzi[2,*], Séverine Planchais[1,*], Delphine De Vos[1,3], Bualuang Faiyue[1,4], Pierre Carol[1], Chedly Abdelly[2] and Arnould Savouré[1,‡]

1Sorbonne Universités, UPMC Univ Paris 06, iEES, UMR 7618, UPMC Paris06 - Sorbonne (UPEC, UPMC, CNRS, IRD, INRA, Paris Diderot), case 237, 4 place Jussieu, F-75252 Paris cedex 05, France

2 Laboratoire des Plantes Extrêmophiles, Centre de Biotechnologie de Borj-Cedria (CBBC), BP 901, Hammam-Lif 2050, Tunisia

3 Present address: Institut Jean-Pierre Bourgin, UMR 1318 INRA-AgroParisTech, Centre INRA Versailles, 78026 Versailles Cedex, France.

4 Present address: Department of Biology, Mahidol Wittayanusorn School, Salaya, Phuttamonthon, Nakhon Pathom 73170, Thailand

* These authors contributed equally to this work

‡ Corresponding author

Telephone: +33 1 44 27 26 72

Fax : +33 1 44 27 35 16

Email: arnould.savoure@upmc.fr

Short running title

Roles of phopholipases Dζ during salt stress in Arabidopsis

Main conclusion

Phospholipases Dζ play different roles in Arabidopsis salt tolerance affecting the regulation of ion transport and antioxidant responses.

Abstract

Lipid signalling mediated by phospholipase D (PLD) plays essential roles in plant growth including stress and hormonal responses. Here we show that *PLDζ1* and *PLDζ2* have distinct effects on Arabidopsis responses to salinity. A transcriptome analysis of a double *pldζ1pldζ2* mutant revealed a cluster of genes involved in abiotic and biotic stresses, such as the high salt stress responsive genes *DDF1* and *RD29A*. Another cluster of genes with a common expression pattern included ROS detoxification genes involved in electron transport and biotic and abiotic stress responses. Total SOD activity was induced early in the shoots and roots of all *pldζ* mutants exposed to mild or severe salinity with the highest SOD activity measured in *pldζ2* at 14 days. Lipid peroxidation in shoots and roots was higher in the *pldζ1* mutant upon salt treatment and *pldζ1* accumulated H_2O_2 earlier than other genotypes in response to salt. Salinity caused less deleterious effects on K^+ accumulation in shoots and roots of the *pldζ2* mutant than of wild type, causing only a slight variation in Na^+/K^+ ratio. Relative growth rates of wild-type plants, *pldζ1, pldζ2* and *pldζ1pldζ2* mutants were similar in control conditions but strongly affected by salt in WT and *pldζ1*. The efficiency of photosystem II, estimated by measuring the ratio of chlorophyll fluorescence (Fv/Fm ratio), was strongly decreased in *pldζ1* under salt stress. In conclusion, *PLDζ2* plays a key role in determining Arabidopsis sensitivity to salt stress allowing ion transport and antioxidant responses to be finely regulated.

Keywords: Ion relations; Phospholipase D; PLDζ; Reactive oxygen species; Salt stress; Transcriptome.

Introduction

Salinity is a major environmental constraint on the growth, productivity and diversity of plants. The effect of salt stress on plants depends on the salt concentration, the duration of exposure and the plant genotype (Ellouzi et al. 2011). The presence of salt in the environment induces water deficit in plants because the external water potential is lowered, while ion toxicity and nutritional alterations disturb ion transport systems (Munns and Tester 2008; Julkowska and Testerink 2015). Salt stress also causes membrane damage, alters levels of growth regulators, inhibits some enzymes, and disrupts photosynthesis, and may thus lead to plant death.

One of the known plant responses to salt stress is ROS production (for review see Miller et al. 2010; Ben Rejeb et al. 2014). Plant cells need to regulate ROS production as excess ROS is potentially harmful to nucleic acids, proteins and lipids, and may therefore lead to cell injury and death (Gill and Tuteja 2010). ROS produced through NAPDH oxidase activity was shown to be mediated by phospholipid signalling (Zhang et al. 2009). The second messenger phosphatidic acid (PA) is a phospholipid which targets specific proteins to bring about cellular and physiological changes that allow plants to adapt to abiotic stresses (for review see Hong et al. 2010; Hou et al. 2016). PA is formed when phospholipase D (PLD) hydrolyses structural phospholipids at the terminal phosphoesteric bond with release of the hydrophilic head group. In plants, phospholipase D (PLD) is predominant among the phospholipase families (for review see Li et al. 2009; McLoughlin and Testerink, 2013). PLD activity increases rapidly in response to various environmental stresses such as cold, drought, and salinity (Vergnolle et al. 2005; Bargmann et al. 2009; Hong et al. 2010). Proline accumulation, another common physiological response to stress, was shown to be negatively regulated by PLD activity in *Arabidopsis thaliana* (Thiery et al. 2004).

In *A. thaliana*, the PLD family includes 12 members that are classified into six types, PLDα (3 isoforms), -β (2 isoforms), -γ (3 isoforms), -δ, -ε, and -ζ (2 isoforms), according to their sequences and enzymatic properties (Bargmann and Munnik 2006). Biochemical studies have revealed that the phospholipid-hydrolysing activities of PLD are either calcium-dependent through a C2 domain (C2-PLD) or calcium-independent having pleckstrin homology (PH) and phox homology (PX) domains (PXPH-PLD) (Meijer and Munnik 2003). Several PLD isoforms have been functionally characterized. The two PLDζs (*PLDζ1* and *PLDζ2*) are structurally different from other PLDs (for review see Li et al. 2009). PLDζ1 and PLDζ2 do not have C2 domains and do not require Ca^{2+} for enzymatic activity (Qin and Wang 2002), but they do have PH and PX domains (Qin and Wang 2002). *PLDζ1* gene expression is five-fold greater in roots than in leaves and the gene function is required for root hair morphogenesis (Li et al. 2006). The *PLDζ2* gene is mainly expressed in roots

(Li et al. 2006). *PLDζ2* gene expression is triggered by exogenous auxin (Li and Xue 2007) and phosphate (Li et al. 2006). PLDζ1 and PLDζ2 were shown to be involved in the process by which root architecture adapts to the lack of phosphate (Li et al. 2006). PLD*ζ2* is also involved in vesicle trafficking and auxin transport (Li and Xue 2007). The *pldζ2* mutant has a reduced halotropic response, i.e. the capacity to change the direction of root growth to avoid salt, due to impaired vesicle trafficking (Galvan-Ampudia et al. 2013).

In this study, the roles of *PLDζ1* and *PLDζ2* were investigated in Arabidopsis responding to salt stress. The global transcriptome of the *pldζ1pldζ2* double mutant treated with salt was analysed to identify candidate genes regulated by these PLDs. Changes in growth, ion balance, ROS content, antioxidants, and lipid peroxidation were compared in wild type, *pldζ1*, *pldζ2*, and *pldζ1pldζ2* after short and long periods of salt treatment. *pldζ1* and *pldζ2* mutants responded differently to salt stress suggesting they have distinct physiological roles in Arabidopsis.

Materials and methods

Plant materials and growth conditions

Arabidopsis thaliana (L.) Heynh ecotype Columbia-0 (Col-0) was used as the wild type in this study and was obtained from Nottingham Arabidopsis Stock Centre, Loughborough, United Kingdom. Homozygous T-DNA insertion mutant lines *pldζ1* (SALK_083090) and pldζ2A (SALK_094369) were obtained from the Salk Institute, La Jolla, USA (Alonso and Stepanova 2003) and have been described by Li et al. (2006). Double homozygous mutant *pldζ1pldζ2* plants were isolated from the F2 progeny of crosses between *pldζ1* and *pldζ2.* The presence and homozygosity of the T-DNA alleles were checked by triplex PCR in all experimental lines using a primer specific to the left border of the T-DNA and two gene-specific primers flanking the insertion site (Suppl. Fig. S1 and Suppl. Table S1).

Surface sterilized seeds of wild-type and mutant lines were sown onto grids placed on Petri dishes containing 0.5 × Murashige and Skoog (MS; Murashige and Skoog 1962) solid medium (0.8 % agar) according to Parre et al. (2007). Seeds were placed in a cold room at 4 °C for 1 day to break dormancy and then transferred to a growth chamber at 22 °C with continuous light (90 µmol photons m^{-2} s^{-1}). Twelve-day-old Arabidopsis seedlings were exposed to 200 mM NaCl for up to 24 h.

For physiological experiments, wild type*,* *pldζ1*, *pldζ2* and *pldζ1pldζ2* seeds were germinated in plastic pots (70 mL) filled with inert sand and watered daily with distilled water for one week. Seedlings of each genotype were then irrigated with Hewitt nutrient solution (Hewitt 1966) for 3 weeks. The experiments were performed in a glasshouse under controlled conditions, photoperiod of 16h/8h (day/night), at 20-25 °C and 65-75 % relative humidity. Four-week-old plants were treated with 75 mM or 150 mM NaCl and collected after 3 h, 24 h and 72 h for short exposure to salt stress and after 7 and 14 days for long exposure to salinity. Non-stressed plants grown without added salt were collected and used as controls.

Transcriptome analysis of the *pldζ1pldζ2* double mutant

Analysis of the *pldζ1pldζ2* transcriptome was conducted at the Unité de Recherche en Génomique Végétale (Evry, France) using the Complete Arabidopsis Transcriptome MicroArray (CATMA) containing 24576 gene-specific tags from Arabidopsis (Crowe et al. 2003). Six biological replicates and 14 dye swaps (technical replicates) were made. Twelve-day-old seedlings treated for 3 h with either 200 mM NaCl or 400 mM mannitol for stress conditions or with 0.5 × MS for control conditions were rapidly washed with water and immediately frozen in liquid nitrogen and stored at

−80 °C. Total RNA was isolated from seedlings by the guanidinium thiocyanate-CsCl purification method (Sambrook et al. 1989). Labelling of cRNAs with Cy3-dUTP or Cy5-dUTP (Perkin-Elmer-NEN Life Science Products, Courtaboeuf, France), hybridization to slides, and scanning were performed as described in Lurin et al. (2004). Methods and data were deposited in CATMA database RS06-01_PLD (http://urgv.evry.inra.fr/cgi-bin/projects/CATdb/consult_expce.pl?experiment_id=113) and GEO (https://www.ncbi.nlm.nih.gov/geo/query/acc.cgi?acc=GSE9459). Statistical analysis of transcriptome data was done as in Planchais et al. (2014).

Reverse transcription PCR and quantitative PCR analysis of gene expression

Total RNA was extracted from 100 mg of homogenized tissue from different genotypes using the RNeasy Plant Mini Kit (Qiagen, Hilden, Germany) following the manufacturer's instructions. RNA was quantified by measuring the absorbance at 260 nm using a Nanovue spectrophotometer (Nanodrop Spectrophotometer ND 1000, Wilmington, DE, USA). RNA was incubated with DNase I (Sigma-Aldrich, Saint-Louis, MO, USA) to eliminate genomic DNA. For reverse transcription, first-strand cDNA was synthesized from 1.5 µg of total RNA using the RevertAid reverse transcriptase kit (Thermo Fisher Scientific Inc., Waltham, MA, USA). Complementary DNAs were amplified using DreamTaq Green polymerase (Thermo Fisher Scientific Inc.) and gene-specific primers (Supplementary Table S1). The *APT1* gene (At1g27450) was used as a positive control for quantifying relative amounts of cDNA. Amplified PCR fragments were separated on 2 % (w/v) agarose gels and visualized by staining with ethidium bromide and analysing the image with GelDoc (Bio-Rad, Hercules, USA). For real-time PCR, 5 µL of diluted cDNA was used with 10 µL of SYBR®GreenqPCR Master Mix (Thermo Fisher Scientific Inc.) and gene-specific primers in an Eppendorf Master cycler® (Eppendorf France SAS, Montesson, France). Critical thresholds (Ct) were determined by using the Eppendorf Master cycler® realplex software and ratios were calculated by using the method described by Pfaffl (2001). For each gene, a standard curve made with dilutions of cDNA pools was used to calculate reaction efficiencies, and the levels of gene transcript were normalized and expressed relative to the amounts observed under control conditions with *APT1* (At1g27450) as housekeeping gene. All semi-quantitative RT-PCR and real-time PCR experiments were carried out with three biological replicates.

Measurements of plant biomass, maximum efficiency of PSII photochemistry, and leaf water status

Fresh weight (FW) and dry weight (DW) of rosettes and roots were measured at each experimental time point to evaluate leaf and root growth. The accumulation of biomass was estimated by determining the relative growth rate (RGR), which is a measure of biomass production relative to

treatment duration and/or initial plant size. RGR was calculated as $\Delta \ln(DW)/\Delta t$, where DW is the dry weight, ln is the natural logarithm and Δ represents the difference between final and initial values for a given time interval Δt (Hunt, 1990). The maximum efficiency of PSII photochemistry (*Fv/Fm*) was monitored throughout the experiment using a portable mini-PAM fluorometer (ADC BioScientific LC pro System Serial, Hoddesdon, UK).

The relative leaf water content (RWC) was calculated as 100×(FW-DW)/(TW-DW), where TW was the turgid weight of leaves saturated for 24 h in deionized water at 4 °C in darkness and DW was obtained after oven-drying the leaves at 60 °C for 72 h according to Ellouzi et al. (2013).

Measurement of ion content

Desiccated leaf and root tissues were ground to a fine powder and then broken down with concentrated 0.5 % HNO_3 according to Deal (1954). Na^+ and K^+ contents were determined using flame emission photometry (Corning, Tewksbury, MA, USA). In emission photometry the soluble mineral component is injected into an air-propane flame. Following thermal excitation a characteristic spectrum of lines is emitted that are selected by monochromator filters. Behind each filter a photoreceptor cell detects the intensity of the emitted light which is proportional to the amount of the emitting element contained in the vaporized solution.

Histochemical detection of hydrogen peroxide

The localization of hydrogen peroxide was determined according to Ben Rejeb et al. (2015). Fresh leaf and root samples were collected from each mutant and infiltrated with a solution containing 0.5 mg ml^{-1} diaminobenzidine (DAB) and 10 mM Mes buffer pH 5.8. Samples were then kept at room temperature until the brown residue generated by H_2O_2-DAB polymerization developed. Samples were incubated for 60 min in boiling ethanol before being photographed.

Measurement of hydrogen peroxide concentration

Fresh leaf and root samples were ground in 0.2 % trichloroacetic acid (TCA) in a mortar and pestle chilled on ice. The homogenate was centrifuged at 15000 *g* for 20 min at 4 °C. The supernatant was mixed with 10 mM sodium phosphate buffer pH 7 and 1 M KI. The H_2O_2 content was determined by comparing the absorbance of the sample at 390 nm with a standard calibration curve, expressing values in µmol H_2O_2 g^{-1} DW.

Membrane lipid peroxidation assays

Levels of lipid peroxidation were assessed by measuring the amount of malondialdehyde (MDA) in tissue. Fresh leaf and root samples were homogenized in 10 % TCA. The homogenate was centrifuged at 15000 *g* for 20 min at 4 °C. The supernatant was collected and mixed with 0.5 % thiobarbituric acid in 20 % TCA. Samples were heated at 95 °C for 25 min in a water bath, and then cooled on ice. The samples were centrifuged at 10000 *g* for 10 min and the absorbance of solutions at 532 and 600 nm was recorded. The MDA level was calculated using the extinction coefficient for MDA [$\varepsilon = 155\ \mu M\ cm^{-1}$] expressed in nmol MDA g^{-1} DW.

Protein extraction and antioxidant enzyme assays

Leaf and root samples of each genotype were homogenized in a chilled mortar containing 10 % (w/w) poly-vinyl-polypyrrolidone in 50 mM potassium phosphate buffer pH 7, 0.1 mM ethylenediaminetetraacetic acid (EDTA) and 1 mM dithiothreitol. Homogenates were then centrifuged at 10000 *g* for 15 min at 4 °C. The supernatants were collected and stored at -20 °C for protein and enzyme assays. The soluble protein content of leaves and roots was estimated according to Bradford (1976) with bovine serum albumin as the standard. Superoxide dismutase (SOD, EC.1.15.1.1) activity was assayed based on the inhibition of nitro blue tetrazolium (NBT) reduction (Beyer and Fridovich 1987). The assay was conducted in 50 mM potassium phosphate pH 7.8 containing 50 µL of enzyme extract, 2.25 mM NBT, 13 mM methionine, 2 mM riboflavin and 1 mM EDTA. The reaction was started by illuminating the sample for 15 min and stopped by switching the light off. The amount of blue formazan formed was determined by measuring the absorbance at 560 nm. One unit of SOD activity (U) was defined as the amount of enzyme that caused 50 % inhibition of NBT reduction.

Statistical analysis

Differences between measurements and between genotypes at different times were evaluated by analysis of variance (one-way ANOVA) using SPSS (Chicago, IL, USA). Differences were considered as statistically significant when $P \leq 0.05$.

Results

Analysis of the *pldζ1pldζ2* double mutant transcriptome

If Arabidopsis PLDζ act in lipid signalling in response to salt stress then a *pldζ1pldζ2* double mutant, lacking both PLDζ and PLDζ2, would be expected to differ from WT in the way it responds to salt stress. We first investigated gene expression in WT after 3 h exposure to salt or mannitol. This was to test whether the ionic stress component of the response could be distinguished from the osmotic stress component. A large common set of genes was induced (560 genes) or repressed (221 genes) by the two individual treatments, which was attributed to the similar effects of osmotic stress on the plants (Supplementary Fig. S2). However a smaller subset of genes was specifically induced (170 genes) or repressed (82 genes) only by salt. For example, the known salt-stress responsive gene *DDF1* was specifically upregulated in response to NaCl in WT but was not affected by hyperosmotic stress caused by mannitol. Global transcriptome analysis of the *pldζ1pldζ2* double mutant also revealed common sets of genes that were triggered or repressed by both NaCl and mannitol, but also differential expression of subsets of genes in a salt-specific and mannitol-specific manner (data not shown). In further experiments we were thus able to distinguish between ionic and osmotic stress effects, focusing on the former. As some genes were differentially and specifically regulated by NaCl, the perception and transduction of the ionic component of the salt stress signal must have occurred within the 3 h of the stress treatment.

We then compared differences in the NaCl stress transcriptomes of *pldζ1pldζ2* and WT with the WT NaCl stress response. In WT genes were either induced (642 genes) or repressed (241 genes) after 3 h salt stress (Fig. 1). Twenty of the salt-induced genes in WT were found to be expressed at lower levels in *pldζ1pldζ2* after 3 h salt treatment than in WT in the same conditions (intersection in Fig. 1a). This cluster of genes induced in WT, but less strongly induced in *pldζ1pldζ2* was defined as cluster 1 (Fig. 1 and Suppl. Fig. S3). Analysis of gene ontology using BAR Classification SuperViewer (http://bar.utoronto.ca) showed an over-representation of genes involved in abiotic and biotic stresses in cluster 1 (Suppl. Fig. S4). It was noted that the salt-stress responsive genes *DDF1* and *RD29A* (Magome et al. 2008) were present in cluster 1. We investigated the expression of these two genes in WT, the *pldζ1* and *pldζ2* single mutants and the *pldζ1pldζ2* double mutant using RT-PCR and quantitative PCR (Fig. 2a, c). The RT-PCR analysis confirmed that *DDF1* expression was induced by salinity in WT plants (Fig. 2a). *DDF1* gene expression was induced in *pldζ1pldζ2* but not as strongly (4.9-fold) as in WT (6-fold) confirming the transcriptome data (Fig. 2c). In comparison, *DDF1* expression was induced 9.7-fold in *pldζ2* and 7.8-fold in *pldζ1* (Fig. 2a, c). Similarly, *RD29A* expression was strongly induced by salt treatment in WT (Fig. 2a, c) but less

so in *pldζ1pldζ2* as expected from the transcriptomic data. Of the four genotypes tested *pldζ2* again showed the highest level of salt-induction with a 10.4-fold increase in *RD29A* expression.

Another cluster of genes, cluster 2, was identified by comparing the differences in the *pldζ1pldζ2* and WT transcriptomes between control and salt stress conditions. In this cluster 23 genes were deregulated in the double mutant in both conditions, 8 upregulated and 15 downregulated (Fig. 1 b, Suppl. Fig. S5). Cluster 2 gene functions mainly related to electron transport and biotic and abiotic stresses (Suppl. Fig. S4). The ROS detoxification genes *SOD1* (At1g08830*)* and *CCS1* (*Copper Chaperone for SOD1,* At1g12520) were overexpressed in *pldζ1pldζ2* compared to WT after salt treatment and in control conditions (Suppl. Fig. S5).

ROS detoxification was impaired in *pldζ* mutants

We verified whether *SOD1* expression was altered in *pldζ* single and double mutants by RT-PCR, and compared it to expression of two other ROS detoxifying genes, ascorbate peroxidase 1 (*APX1*) and catalase (*CAT2*), which are commonly used as oxidative burst markers (Fig. 2b). *APX1* expression was slightly higher in *pldζ2* than in WT and *pldζ1*, but was lower in *pldζ1pldζ2*. *SOD1* gene expression was upregulated by salt treatment in both *pldζ* single mutants but not in WT. Expression of *CAT2* was highest in *pldζ2* compared to the other genotypes even in control conditions (Fig. 2).

To test whether the lack of both or either PLDζ affected the ROS detoxification activity of SOD, SOD activity was monitored for 14 days in the shoots and roots of WT and *pldζ* mutants exposed to moderate (75 mM NaCl) or severe salinity (150 mM NaCl) (Fig. 3). In leaves treated with 75 mM NaCl SOD activity increased transiently in the first 72 h up to 316 % in WT, 169 % in *pldζ1* and 108 % in *pldζ1pldζ2*, declining less rapidly then remaining constant until the end of the time course. In roots, the kinetics of SOD activity were markedly different in *pldζ1pldζ2* in comparison to other genotypes as the sharp transient increase occurred within the first three days of mild salt treatment (Fig. 3). Under the same salt conditions, no significant variations were detected in stressed roots of WT and *pldζ1* mutants. By contrast SOD activity in both the shoots and roots of *pldζ2* treated with 75 mM NaCl increased linearly to reach a plateau that remained higher than levels in the other genotypes at the end of the 14-day experiment. Upon severe NaCl stress, SOD activity in leaves of *pldζ2* and *pldζ1pldζ2* mutants showed a distinct profile with a transient maximum activity at 3 h, remaining higher than that of WT and *pldζ1* mutants until the end of the salt treatment (Fig. 3). No substantial changes in SOD activity were observed in shoots of WT and *pldζ1* mutants during stress from 150 mM NaCl. SOD activities increased distinctly in the roots of all genotypes except *pldζ1* under severe salt stress. Although there was a transient maximal peak in SOD activity in WT during

the first 72 h of exposure to 150 mM NaCl, the highest SOD activities were measured in *pldζ2* and *pldζ1pldζ2* mutants after 14 days.

pldζ mutants differentially accumulate ROS in response to salt stress

The presence of H_2O_2 is an indicator of oxidative stress. The differential accumulation of H_2O_2 in leaves and roots over the duration of the stress was evaluated in the four genotypes using DAB, which stains tissues brown in the presence of H_2O_2 (Fig. 4). Leaves and roots grown in the absence of salt did not stain brown with DAB. After 3 h salt treatment, whole leaves and roots of WT and *pldζ1pldζ2* and *pldζ1* were stained brown with DAB (Fig. 4). Although the assay is qualitative, the intensity of the staining consistently increased over the duration of the experiment. Roots and shoots of *pldζ2* mutant were the most faintly stained, indicating these tissues had the lowest amounts of H_2O_2.

The differences observed in DAB staining in *pldζ* mutants led us to quantify H_2O_2 content. H_2O_2 measurements corresponded with the DAB staining. In the absence of salt stress, H_2O_2 did not accumulate above basal levels in any of the four genotypes. Under mild salt stress, H_2O_2 content increased steadily in shoots and roots in all four genotypes, accumulating faster during the first 24 h (Fig. 5). H_2O_2 accumulated at a similar rate in WT and *pldζ1*, but *pldζ2* and *pldζ1pldζ2* accumulated less than half of the amount measured in WT (Fig. 5). Under severe salt stress, *pldζ2* leaves and roots had the lowest levels of H_2O_2 compared to the other *pldζ* genotypes.

Oxidative stress can lead to damage of structural macromolecules including lipids. Lipid peroxidation in leaves and roots was estimated by quantifying malondialdehyde (MDA), which forms when ROS attack lipids. The accumulation of MDA greatly increased in both leaves and roots growing under salt stress (Fig. 6). However the genotypes accumulated MDA differently. The highest amounts of MDA were found in leaves and roots of salt-stressed *pldζ1*, while *pldζ2* accumulated the least MDA in leaves and roots in response to both moderate and severe salt stresses (Fig. 6).

Ion distribution was altered in *pldζ* mutants responding to salt stress

The distribution of ions between leaves and roots of WT and the *pldζ* mutants exposed to 14 days of either moderate or severe salinity is shown in Table 1. Changes in Na^+ and Cl^- content followed the same profile over the 14 days in all genotypes and under both salt treatments, increasing linearly (data not shown) and reaching high levels by the end of the experiment. These final levels were higher in roots than in leaves (Table 1). There were some differences between genotypes. *pldζ1* mutants stressed by 150 mM NaCl had the most Na^+ in leaves (7.3 mmol g^{-1} DW) and roots (8.4

mmol g^{-1} DW) (Table 1). This increase was concomitant with the highest Cl^- accumulation, which was greater in roots (5.8 mmol g^{-1}DW) than in leaves (3.9 mmol g^{-1} DW) (Table 1). However, Na^+ content increased more than Cl^- content within leaves and roots upon salt stress. When grown in 150 mM NaCl, *pldζ2* mutants contained the least Na^+ (3 mmol g^{-1} DW in leaves and 3.9 mmol g^{-1} DW in roots) (Table 1) and the least Cl^- (2.1 mmol g^{-1} DW in leaves and 3.1 mmol g^{-1} DW in roots). Na^+ accumulation concomitant with K^+ loss was higher in roots than in leaves in all genotypes under salt stress (Table 1). Salt-stressed *pldζ1* mutants showed the most drastic decrease in K^+ content with 6-fold and 22-fold decreases in leaves and roots, respectively, when treated with 150 mM NaCl (Table 1). By contrast, only a slight variation in Na^+/K^+ ratio was observed in *pldζ2* mutant. Salinity effects on K^+ accumulation were less severe in shoots (2-fold decrease) and roots (7-fold decrease) in *pldζ2* than in other genotypes.

Relative growth rate, relative water content and efficiency of chlorophyll fluorescence in *pldζ* mutants during salt stress

Relative growth rate (RGR) of WT, *pldζ1*, *pldζ2* and *pldζ1pldζ2* had decreased after 14 days of exposure to NaCl (Fig. 7). RGRs of *pldζ1pldζ2* and *pldζ2* mutants were less affected by salt than those of *pldζ1* and WT, which were severely inhibited by even mild salt stress. By measuring the change in relative water content (RWC) over time, we found that salt stress induced dehydration in leaves of all genotypes (Fig. 8). *pldζ1* mutants became the most dehydrated with RWC decreases of 50 % in 75 mM NaCl and 66 % in 150 mM NaCl compared to the same genotype at the same developmental stage in control conditions (Fig. 8). The *pldζ1pldζ2* leaves only lost 40 % of RWC compared to plants grown in control conditions.

The *Fv/Fm* ratio is a convenient measure of photosynthesis efficiency at the photosystem II level (PSII). The *Fv/Fm* ratios for all genotypes were constant in control conditions but decreased under salt stress (Fig. 8). After 14 days of salt treatment, the *Fv/Fm* ratios of *pldζ1* plants had decreased by as much as 64 % in 150 mM NaCl. By contrast *pldζ1pldζ2* plants maintained higher *Fv/Fm* ratio values, which were 1.16 and 1.32-fold higher than those measured in WT, respectively under mild and severe stress, suggesting PSII functions better under stress in the absence of PLDζ (Fig. 8).

Discussion

Recent studies have provided valuable insights into the molecular and cellular mechanisms by which plants respond to and tolerate salinity stress (Deinlein et al. 2014; Julkowska and Testerink 2015; Slama et al. 2015). Although *Arabidopsis thaliana* is considered to be a glycophyte, it has

been widely used as a genetic model to investigate salt signalling mechanisms. Salt treatment significantly inhibits growth of *A. thaliana* with intracellular Na^+ concentration increasing at the expense of K^+ (Ghars et al. 2008; Ellouzi et al. 2011). The replacement of K^+ by Na^+ affects the cell's Na^+-sensitive enzymes, including components of the photosynthetic machinery, that determine plant growth and yield. Tolerance to salt stress depends on complex signalling networks enabling plants to respond rapidly and efficiently to this constraint (Zhu 2002). Many signal transduction pathways have been shown to be stimulated in response to high salinity (Bragmann et al. 2009; Julkowska and Testerink 2015). Lipid mediators are key components in the signalling network of plant stress adaptation, including adaptation to salinity (Julkowska and Testerink 2015). As an enzyme responsible for producing PA, we focused on the roles of the two *A. thaliana* PLDζ in salt tolerance.

To identify changes in gene expression affected by PLDζ activity, the transcriptome of a double *pldζ1pldζ2* mutant was compared to the WT transcriptome. In gene cluster 1, the stress-responsive genes *DDF1* and *RD29A* (Thiery et al. 2004; Magome et al. 2004; Magome et al. 2008) were strongly induced by severe salt stress (200 mM NaCl) within 3 h in the WT but were less strongly induced in *pldζ1pldζ2* under the same conditions. Transgenic Arabidopsis lines overexpressing *DDF1* were shown to have increased tolerance to high salt stress (170 mM NaCl) by repressing plant growth through the induction of genes coding gibberellin (GA) deactivating enzymes (Magome et al. 2004; Magome et al. 2008). We found that the *pldζ2* single mutant showed higher expression of *DDF1* and *RD29A* under salt stress compared with the WT and other *pldζ* mutants (Fig. 2). The expression of auxin-responsive genes such as *IAA5*, *IAA19*, and *GH3-3* was previously found to be reduced in *pldζ2* mutants of Arabidopsis in response to external IAA (Li and Xue 2007). Therefore, *PLDζ2* may be specifically involved in the regulation of gene expression in stress responses and hormonal signalling for growth. Controlled growth reduction may be an effective strategy to save energy and minimize ROS accumulation while facing the deleterious impact of salt stress (Rangani et al. 2016).

Transcriptomic analysis revealed a second gene cluster that included ROS detoxification genes such as *SOD1* and *CCS1*, which were overexpressed in *pldζ1pldζ2* mutants (Suppl. Fig. S5). It is known that ROS act as second messengers in intracellular signalling cascades to trigger plant tolerance to various abiotic and biotic stresses (Ben Rejeb et al. 2014; Mittler, 2016). When *Cakile maritima*, a salt-tolerant plant, is treated with salt, there is a transient and rapid increase in SOD activity and H_2O_2 content within 4 h. The SOD activity measured in *C. maritima* was eight-fold higher than was found in Arabidopsis (Ellouzi et al. 2013). In the present study, the highest *SOD1*, *CAT2* and *APX* gene expression was observed in *pldζ2* mutant under salt stress (Fig. 2). High expression of *SOD*

under salt stress corresponded with high SOD activity and low H_2O_2 levels in leaves and roots of *pldζ2* mutants, indicating that *PLDζ2* participates in the regulation of ROS generation upon salt stress in Arabidopsis. Several reports show that different PLD family enzymes function in concert with ROS to mediate tolerance responses to various abiotic stresses (Hong et al. 2010, Singh et al. 2012). For example, mutation in *PLDα1* leads to PA deficiency, reduced plasma membrane NADPH oxidase activity, and less ROS in stomata guard cells in response to abscisic acid (Zhang et al. 2009). As a consequence, *pldα1* mutants can not fully close stomata leading to increased water loss (Zhang et al. 2009). We found that *pldζ1* mutants accumulated H_2O_2 faster in leaves and roots than *pldζ2* mutants do in response to salt stress. Moreover, *pldζ1* plants displayed the lowest SOD activity which, associated with the highest levels of H_2O_2, implies that *pldζ1* is more sensitive to salt stress than WT and the other *pldζ* mutants. Interestingly other *pld* mutants such as *pldα1, pldα3* and *pldδ* have also been shown to be hypersensitive to salt treatment (Hong et al. 2008; Bargmann et al. 2009).

Salinity had several striking effects on physiological indexes with distinctions becoming clear between WT and *pldζ1* versus *pldζ2* and *pldζ*1*pldζ2*. The *pldζ1* mutant showed the highest Na^+ content in leaves and roots compared with the other genotypes upon salt stress, leading to a drastic decrease in K^+ content in roots and shoots (Table 1). The loss of K^+ could be explained by downregulation of the expression of genes involved in K^+ transport like the HAK5 transporter gene. HAK5 is expressed under the control of *DDF2* gene, a transcription factor which is homologous to *DDF1* (Hong et al. 2013). The massive K efflux could also be mediated by the opening of outward-rectifying depolarisation-activated (GORK) channels, an outward K^+ channel (for review see Anschütz et al., 2014). Phospholipase Dζ could be involved in the regulation of ion channels by modulating their lipid environment. For example in yeast cells, many ion channels have been shown to be located in plasma membrane microdomains called lipid rafts with channel activities dependent on the lipid raft composition (for review see Mollinedo 2012).

RGR measurements showed that WT and *pldζ1* have only a limited capacity to withstand the presence of salt. Sensitivity of WT and *pldζ1* to salt stress was associated with a decline in the leaf water content, increase in Na^+ and Cl^- preferentially accumulated in roots, early induction of oxidative stress (excess H_2O_2 and MDA), and inhibition of photosynthesis from the toxicity of the salt ions (low *Fv/Fm* ratio). For most markers *pldζ1* was more sensitive than WT, indicating that PLDζ1 is required in the regulation of growth in normal conditions. Interestingly and as described by Ohashi et al. (2003) and Chen et al. (2013), this PLD isoform is greatly involved in the root development and growth and the lack of this PLD may lead to enhanced salt stress sensitivity (Wang, 2005).

Conversely, *pldζ2* mutants tolerated salt stress better than WT. This response may be related to its ability to minimize redistribution of Na^+ and Cl^- to the roots, resulting in the lowest Na^+/K^+ ratio and consequently better retention of K^+ in these organs. *pldζ2* grew less than *pldζ1 pldζ2* double mutant, which produced more biomass in both roots and leaves. We can consider growth reduction in *pldζ2* to be a strategy to maintain performance under salinity by first controlling ion homeostasis. The activation of the Salt Overly Sensitive (SOS) signalling pathway is a key mechanism for Na^+ exclusion in roots (Zhu, 2000). PLDs were shown to interact strongly with SOS and plasma membrane transporters under salt stress (Yu et al. 2010). Notably, the activation of PLD in salt stressed tobacco elevated the PA level which is a direct stimulator of SOS1, a central regulator of ion homeostasis (Gardiner et al. 2001). Other studies suggested that there is a functional connection between the activation of *PLDζ2* and SOS3, which is more prominent in the roots and has a crucial role in Na^+/K^+ dynamics (Muzi et al. 2016). Much less is known about the cross-talk between PLD and SOS signalling pathways under salt stress. However, the above findings will guide future research to elucidate the mechanism of the salt tolerance in *pldζ2*.

It was clear from our results that the *pldζ2* mutant was the most tolerant of salt stress as evidenced by the lowest Na^+/K^+ ratio. It has long been known that salinity stress triggers a dramatic increase in ROS accumulation in plant tissues. Interestingly, our results showed that salt-stressed *pldζ2* plants also displayed the lowest levels of H_2O_2 and MDA detected in both leaves and roots. In addition, mild and severe salt stresses triggered higher SOD activity in *pldζ2* than in the other genotypes which could explain why H_2O_2 and MDA levels were lower in both leaves and roots. The oxidative burst indicators SOD, H_2O_2 and MDA indicate the presence of an efficient antioxidant defence in *pldζ2* mutant. The lack of PLDζ2 may therefore allow a better performance of the plants facing moderate and severe salinity due to a primed antioxidant defence system.

In conclusion, our study suggests that in Arabidopsis *PLDζ* genes encode isoforms that have distinct roles in plant growth particularly under salt stress. The *pldζ2* KO mutant was more salt-tolerant than the WT as growth, water status, ion homeostasis and antioxidant defence systems were all better adjusted to withstanding salinity. Possibly *pldζ* are differently regulated in halophytes enabling them to tolerate salinity. Looking for natural variants or mutations in *PLDζ2* gene might be a way to improve salt tolerance in glycophytic crops.

Author contribution statement

AS and CA conceived and designed the research. Data collection, analysis and interpretation were performed by AO, HE, SP and BF. SP conducted the transcriptomic analysis. DDV was involved in

the molecular analysis of *pldζ* mutant and in obtaining the double *pldζ1pldζ2* mutant. PC contributed to study conception and design. AO, HE, SP wrote the manuscript. AS and CA supervised manuscript preparation and correction. All authors read and approved the manuscript.

Acknowledgments

This work was supported by the UPMC (France) and the CBBC (Tunisia) and also supported by the Tunisian-French UTIQUE network (n°13G0929). We thank Frederique Bitton and Jean-Pierre Renou from URG-INRA, Evry (France) for help producing the microarray data. Bualuang Faiyue thanks the Junior Research Fellowship Program supported by the French Embassy in Thailand.

References

Alonso JM, Stepanova AN (2003) T-DNA mutagenesis in Arabidopsis. Methods Mol Biol Clifton NJ 236:177–188. doi: 10.1385/1-59259-413-1:177

Anschütz U, Becker D, Shabala S (2014) Going beyond nutrition: regulation of potassium homoeostasis as a common denominator of plant adaptive responses to environment. J Plant Physiol 171:670-687.

Bargmann BO, Laxalt AM, Riet BT, Testerink C, Merquiol E, Mosblech A, Leon-Reyes A, Pieterse CM, Haring MA, Heilmann I, Bartels D, Munnik T (2009) Reassessing the role of phospholipase D in the *Arabidopsis* wounding response. Plant Cell Environ 32 743-757. doi: 10.1111/j.1365-3040.2009.01962.x

Bargmann BO, Munnik T (2006) The role of phospholipase D in plant stress responses. Curr Opin Plant Biol 9:515–22. doi: 10.1016/j.pbi.2006.07.011

Ben Rejeb K, Abdelly C, Savouré A (2014) How reactive oxygen species and proline face stress together. Plant Physiol Biochem 80:278–284. doi: 10.1016/j.plaphy.2014.04.007

Ben Rejeb K, Lefebvre-De Vos D, Le Disquet I, Leprince A-S, Bordenave M, Maldiney R, Jdey A, Abdelly C, Savouré A (2015) Hydrogen peroxide produced by NADPH oxidases increases proline accumulation during salt or mannitol stress in *Arabidopsis thaliana*. New Phytol 208:1138–1148. doi: 10.1111/nph.13550

Beyer WF, Fridovich I (1987) Assaying for superoxide dismutase activity: Some large consequences of minor changes in conditions. Anal Biochem 161:559–566. doi: 10.1016/0003-2697(87)90489-1

521 Bradford MM (1976) A rapid and sensitive method for the quantitation of microgram quantities of
522 protein utilizing the principle of protein-dye binding. Anal Biochem 72:248–54.
523 Bargmann BO, Laxalt AM, Riet BT, van Schooten B, Merquiol E, Testerink C, Haring MA, Bartels
524 D, Munnik T (2009) Multiple PLDs required for high salinity and water deficit tolerance in
525 plants. Plant Cell Physiol 50:78-89. doi: 10.1093/pcp/pcn173
526 Chen MX, Lung SC, Du ZY, Chye ML (2013) Engineering plants to tolerate abiotic stresses.
527 Biocatal Agric Biotechnol 3:81-87. doi: 10.1016/j.bcab.2013.09.010
528 Crowe ML, Serizet C, Thareau V, Aubourg S, Rouzé P, Hilson P, Beynon J, Weisbeek P, van
529 Hummelen P, Reymond P, Paz-Ares J, Nietfeld W, Trick M (2003) CATMA: a complete
530 Arabidopsis GST database. Nucleic Acids Res 31:156–158.
531 Deal SB (1954) Flame photometric determination of sodium and potassium. Anal Chem 26:598–
532 599. doi: 10.1021/ac60087a063
533 Deinlein U, Stephan AB, Horie T, Luo W, Xu G, Schroeder JI (2014) Plant salt-tolerance
534 mechanisms. Trends Plant Sci 19:371–379. doi: 10.1016/j.tplants.2014.02.001
535 Ellouzi H, Ben Hamed K, Cela J, Munné-Bosch S, Abdelly C (2011) Early effects of salt stress on
536 the physiological and oxidative status of *Cakile maritima* (halophyte) and *Arabidopsis thaliana*
537 (glycophyte). Physiol Plant 142:128–143. doi: 10.1111/j.1399-3054.2011.01450.x
538 Ellouzi H, Ben Hamed K, Asensi-Fabado MA, Müller M, Abdelly C, Munné-Bosch S (2013)
539 Drought and cadmium may be as effective as salinity in conferring subsequent salt stress tolerance
540 in *Cakile maritima*. Planta 237:1311–1323. doi: 10.1007/s00425-013-1847-7
541 Galvan-Ampudia CS, Julkowska MM, Darwish E, Gandullo J, Korver RA, Brunoud G, Haring MA,
542 Munnik T, Vernoux T, Testerink C (2013) Halotropism is a response of plant roots to avoid a saline
543 environment. Curr Biol 23:2044–2050. doi: 10.1016/j.cub.2013.08.042
544 Gardiner JC, Harper JD, Weerakoon ND, Collings DA, Ritchie S, Gilroy S, Cyr RJ, Marc J (2001)
545 A 90-kD phospholipase D from tobacco binds to microtubules and the plasma membrane. Plant Cell
546 13: 2143–2158.
547 Ghars MA, Parre E, Debez A, Bordenave M, Richard L, Leport L, Bouchereau A, Savoure A,
548 Abdelly C (2008) Comparative salt tolerance analysis between Arabidopsis thaliana and
549 *Thellungiella halophila*, with special emphasis on K^+/Na^+ selectivity and proline accumulation. J
550 Plant Physiol 165:588–599. doi: 10.1016/j.jplph.2007.05.014
551 Gill SS, Tuteja N (2010) Reactive oxygen species and antioxidant machinery in abiotic stress
552 tolerance in crop plants. Plant Physiol Biochem 48:909–930. doi: 10.1016/j.plaphy.2010.08.016
553 Hewitt E (1966) The composition of the nutrient solution. Sand Water Cult Methods Used Study
554 Plant Nutr 187–246.

555 Hong J-P, Takeshi Y, Kondou Y, Schachtman DP, Matsui M, Shin R (2013) Identification and
556 characterization of transcription factors regulating Arabidopsis *HAK5*. Plant Cell Physiol 54:1478–
557 1490. doi: 10.1093/pcp/pct094
558 Hong Y, Pan X, Welti R, Wang X (2008) Phospholipase Dalpha3 is involved in the hyperosmotic
559 response in Arabidopsis. Plant Cell 20:803–816. doi: 10.1105/tpc.107.056390
560 Hong Y, Zhang W, Wang X (2010) Phospholipase D and phosphatidic acid signalling in plant
561 response to drought and salinity. Plant Cell Env 33:627–635.
562 Hou Q, Ufer G, Bartels D (2016) Lipid signalling in plant responses to abiotic stress. Plant Cell
563 Environ 39:1029–1048. doi: 10.1111/pce.12666
564 Hunt R (1990) Basic Growth analysis: Plant growth analysis for beginners. Unwin Hyman. London.
565 Julkowska MM, Testerink C (2015) Tuning plant signaling and growth to survive salt. Trends Plant
566 Sci 20:586–594. doi: 10.1016/j.tplants.2015.06.008
567 Li G, Xue H-W (2007) Arabidopsis PLDzeta2 regulates vesicle trafficking and is required for auxin
568 response. Plant Cell 19:281–295. doi: 10.1105/tpc.106.041426
569 Li M, Hong Y, Wang X (2009) Phospholipase D- and phosphatidic acid-mediated signaling in
570 plants. Biochim Biophys Acta - Mol Cell Biol Lipids 1791:927–935. doi:
571 10.1016/j.bbalip.2009.02.017
572 Li M, Qin C, Welti R, Wang X (2006) Double knockouts of phospholipases Dzeta1 and Dzeta2 in
573 Arabidopsis affect root elongation during phosphate-limited growth but do not affect root hair
574 patterning. Plant Physiol 140:761–770. doi: 10.1104/pp.105.070995
575 Lurin C, Andrés C, Aubourg S, Bellaoui M, Bitton F, Bruyère C, Caboche M, Debast C, Gualberto
576 J, Hoffmann B, Lecharny A, Ret ML, Martin-Magniette M-L, Mireau H et al (2004) Genome-wide
577 analysis of Arabidopsis pentatricopeptide repeat proteins reveals their essential role in organelle
578 biogenesis. Plant Cell 16:2089–2103. doi: 10.1105/tpc.104.022236
579 Magome H, Yamaguchi S, Hanada A, Kamiya Y, Oda K (2004) *dwarf and delayed-flowering 1*, a
580 novel *Arabidopsis* mutant deficient in gibberellin biosynthesis because of overexpression of a
581 putative AP2 transcription factor. Plant J 37:720-729.
582 Magome H, Yamaguchi S, Hanada A, Kamiya Y, Oda K (2008) The DDF1 transcriptional activator
583 upregulates expression of a gibberellin-deactivating gene, *GA2ox7*, under high-salinity stress in
584 Arabidopsis. Plant J 56:613–626. doi: 10.1111/j.1365-313X.2008.03627.x
585 McLoughlin, F, Testerink C (2013) Phosphatidic acid, a versatile water-stress signal in roots. Front
586 Plant Sci 4: 525. doi: 10.3389/fpls.2013.00525
587 Meijer HJ, Munnik T (2003) Phospholipid-based signaling in plants. Annu Rev Plant Biol 54:265–
588 306.

589 Miller G, Suzuki N, Ciftci-Yilmaz S, Mittler R (2010) Reactive oxygen species homeostasis and
590 signalling during drought and salinity stresses. Plant Cell Environ 33:453–467. doi: 10.1111/j.1365-
591 3040.2009.02041.x
592 Mittler R (2016) ROS are good. Trends Plant Sci 22:11-19 doi: 10.1016/j.tplants.2016.08.002
593 Mollinedo F (2012) Lipid raft involvement in yeast cell growth and death. Front Oncol 2, 140.
594 Munns R, Tester M (2008) Mechanisms of salinity tolerance. Annu Rev Plant Biol 59:651–681. doi:
595 10.1146/Annurev.Arplant.59.032607.092911
596 Murashige T, Skoog F (1962) A revised medium for rapid growth and bio assays with tobacco
597 tissue culture. Physiol Plant 15:473–497.
598 Muzi C, Camoni L, Visconti S, Aducci P (2016) Cold stress affects HC- ATPase and phospholipase
599 D activity in Arabidopsis. Plant Physiol. Biochem.108:328–336.
600 Ohashi Y, Oka A, Rodrigues-Pousada R, Possenti M, Ruberti I, Morelli G, Aoyama T (2003)
601 Modulation of phospholipid signaling by GLABRA2 in root-hair pattern formation. Science.
602 300:1427-30.
603 Parre E, Ghars MA, Leprince AS, Thiery L, Lefebvre D, Bordenave M, Richard L, Mazars C,
604 Abdelly C, Savouré A (2007) Calcium signaling via phospholipase C is essential for proline
605 accumulation upon ionic but not nonionic hyperosmotic stresses in Arabidopsis. Plant Physiol
606 144:503–12. doi: 10.1104/pp.106.095281
607 Pfaffl MW (2001) A new mathematical model for relative quantification in real-time RT–PCR.
608 Nucleic Acids Res 29:e45. doi: 10.1093/nar/29.9.e45
609 Planchais S, Cabassa C, Toka I, Justin A-M, Renou J-P, Savouré A, Carol P (2014) BASIC AMINO
610 ACID CARRIER 2 gene expression modulates arginine and urea content and stress recovery in
611 Arabidopsis leaves. Front Plant Sci 5:330. doi: 10.3389/fpls.2014.00330
612 Qin C, Wang X (2002) The Arabidopsis phospholipase D family. Characterization of a calcium-
613 independent and phosphatidylcholine-selective PLDzeta1 with distinct regulatory domains. Plant
614 Physiol 128:1057–68.
615 Rangani J, Parida AK, Panda A, Kumari A (2016) Coordinated changes in antioxidative enzymes
616 protect the photosynthetic machinery from salinity induced oxidative damage and confer salt
617 tolerance in an extreme halophyte *Salvadora persica* L. Front Plant Sci 7:50. doi:
618 10.3389/fpls.2016.00050
619 Sambrook J, Fritsch EF, Maniatis T (1989) Molecular cloning. Cold Spring Harbor Laboratory
620 Press New York

621 Singh A, Pandey A, Baran wal V, Kapoor S, Pandey GK (2012) Comprehensive expression analysis
622 of rice phospholipase D gene family during abiotic stress and development. Plant Signal Behav 7:
623 847-855.
624 Slama I, Abdelly C, Bouchereau A, Flowers T, Savouré A (2015) Diversity, distribution and roles
625 of osmoprotective compounds accumulated in halophytes under abiotic stress. Ann Bot 115:433–
626 447. doi: 10.1093/aob/mcu239
627 Thiery L, Leprince AS, Lefebvre D, Ghars MA, Debarbieux E, Savouré A (2004) Phospholipase D
628 is a negative regulator of proline biosynthesis in *Arabidopsis thaliana*. J Biol Chem 279:14812–8.
629 Vergnolle C, Vaultier M-N, Taconnat L, Renou J-P, Kader J-C, Zachowski A, Ruelland E (2005)
630 The cold-induced early activation of phospholipase C and D pathways determines the response of
631 two distinct clusters of genes in Arabidopsis cell suspensions. Plant Physiol 139:1217–1233. doi:
632 10.1104/pp.105.068171
633 Wang X (2005) Regulatory functions of phospholipase D and phosphatidic acid in plant growth,
634 development, and stress responses. Plant Physiol 139:566–573.
635 Yu L, Nie J, Cao C, Jin Y, Yan M, Wang F, Liu J, Xiao Y, Liang Y, Zhang W (2010) Phosphatidic
636 acid mediates salt stress response by regulation of MPK6 in *Arabidopsis thaliana*. New Phytol
637 188:762–773.
638 Zhang Y, Zhu H, Zhang Q, Li M, Yan M, Wang R, Wang L, Welti R, Zhang W, Wang X (2009)
639 Phospholipase Dα1 and phosphatidic acid regulate NADPH oxidase activity and production of
640 reactive oxygen species in ABA-mediated stomatal closure in Arabidopsis. Plant Cell 21:2357–
641 2377. doi: 10.1105/tpc.108.062992
642 Zhu JK (2002). Salt and drought stress signal transduction in plants. Annu. Rev. Plant. Biol. 53:
643 247–273.
644 Zhu JK (2000) Genetic analysis of plant salt tolerance using Arabidopsis. Plant Physiol 124:941-8.
645

646

Table 1. Ion content (mmol g^{-1} DW) of leaves and roots of WT and *pldζ1, pldζ2* and *pldζ1pldζ2* mutants after 14 days of mild or severe salt stress. Data are means of three replicates ± S.E. Means indicated by the same superscript letters are not significantly different at $P \leq 0.05$ in one-way ANOVA.

Leaves

	Genotype	WT	*pldζ1*	*pldζ2*	*pldζ1pldζ2*
NaCl (mM)	Ion content				
0	Na^+	0.14 ± 0.01 ^{a}	0.14 ± 0.00 ^{ab}	0.14 ±0.01 ^{ab}	0.15 ± 0.00 ^{b}
75	Na^+	2.36 ± 1.09 ^{b}	3.30 ± 0.91 ^{d}	1.33 ± 0.19 ^{a}	2.89 ± 0.87 ^{c}
150	Na^+	4.50 ± 1.06 ^{c}	7.31 ± 1.06 ^{d}	3.00 ± 1.10 ^{a}	3.92 ± 1.08 ^{b}
0	K^+	2.79 ± 0.24 ^{b}	1.86 ± 0.02 ^{a}	2.32 ± 0.21 ^{ab}	2.07 ± 0.17 ^{a}
75	K^+	1.33 ± 0.15 ^{b}	0.76 ± 0.03 ^{a}	1.30 ± 0.27 ^{b}	0.65 ± 0.01 ^{a}
150	K^+	0.77 ± 0.05 ^{b}	0.31 ± 0.00 ^{a}	1.12 ± 0.22 ^{b}	0.28 ± 0.02 ^{a}
0	Cl^-	0.03 ± 0.00 ^{a}	0.03 ± 0.00 ^{a}	0.09 ± 0.01 ^{b}	0.02 ± 0.00 ^{a}
75	Cl^-	2.37 ± 0.55 ^{c}	2.14 ± 0.32 ^{a}	1.66 ± 0.32 ^{b}	1.70 ± 0.09 ^{a}
150	Cl^-	3.08 ± 0.85 ^{b}	3.88 ± 0.66 ^{d}	2.09 ± 0.53 ^{a}	3.23 ± 1.021 ^{c}
0	Na^+/K^+	0.04 ± 0.00 ^{a}	0.07 ± 0.00 ^{c}	0.06 ± 0.00 ^{b}	0.07 ± 0.00 ^{c}
75	Na^+/K^+	1.80 ± 0.06 ^{b}	4.38 ± 0.19 ^{c}	1.05 ± 0.11 ^{a}	4.56 ± 0.30 ^{c}
150	Na^+/K^+	5.88 ± 0.44 ^{b}	23.88 ± 0.22 ^{d}	2.88 ± 0.51 ^{a}	14.30 ± 1.40 ^{c}
Roots					
0	Na^+	0.12 ± 0.00 ^{a}	0.11 ± 0.01 ^{a}	0.22 ± 0.01 ^{b}	0.13 ± 0.00 ^{a}
75	Na^+	3.73 ± 1.11 ^{b}	3.72 ± 1.19 ^{b}	2.91 ± 0.66 ^{a}	2.89 ± 0.97 ^{a}
150	Na^+	6.43 ± 1.31 ^{b}	8.42 ± 1.16 ^{c}	3.92 ± 0.91 ^{a}	5.88 ± 1.08 ^{b}
0	K^+	1.14 ± 0.21 ^{b}	0.65 ± 0.24 ^{a}	0.98 ± 0.07 ^{ab}	0.94 ± 0.02 ^{ab}
75	K^+	0.40 ± 0.01 ^{c}	0.10 ± 0.00 ^{a}	0.52 ± 0.02 ^{d}	0.28 ± 0.00 ^{b}
150	K^+	0.09 ± 0.01 ^{b}	0.04 ± 0.00 ^{a}	0.15 ± 0.00 ^{c}	0.08 ± 0.00 ^{b}
0	Cl^-	0.04 ± 0.00 ^{a}	0.03 ± 0.00 ^{a}	0.06 ± 0.01 ^{b}	0.03 ± 0.00 ^{a}
75	Cl^-	4.10 ± 0.91 ^{c}	4.08 ± 0.90 ^{c}	1.91 ± 0.36 ^{a}	3.50 ± 0.33 ^{b}
150	Cl^-	5.08 ± 1.05 ^{c}	5.72 ± 0.28 ^{d}	3.00 ± 0.83 ^{a}	4.00 ± 0.83 ^{b}
0	Na^+/K^+	0.11 ± 0.00 ^{a}	0.21 ± 0.06 ^{ab}	0.23 ± 0.01 ^{b}	0.13 ± 0.01 ^{ab}
75	Na^+/K^+	9.61 ± 0.52 ^{b}	35.14 ± 2.75 ^{c}	5.54 ± 0.13 ^{a}	10.22 ± 1.05 ^{b}
150	Na^+/K^+	70.67 ± 2.81 ^{b}	246.95 ± 40.1 ^{d}	55.41 ± 20.0 ^{a}	72.91 ± 1.30 ^{c}

Figures

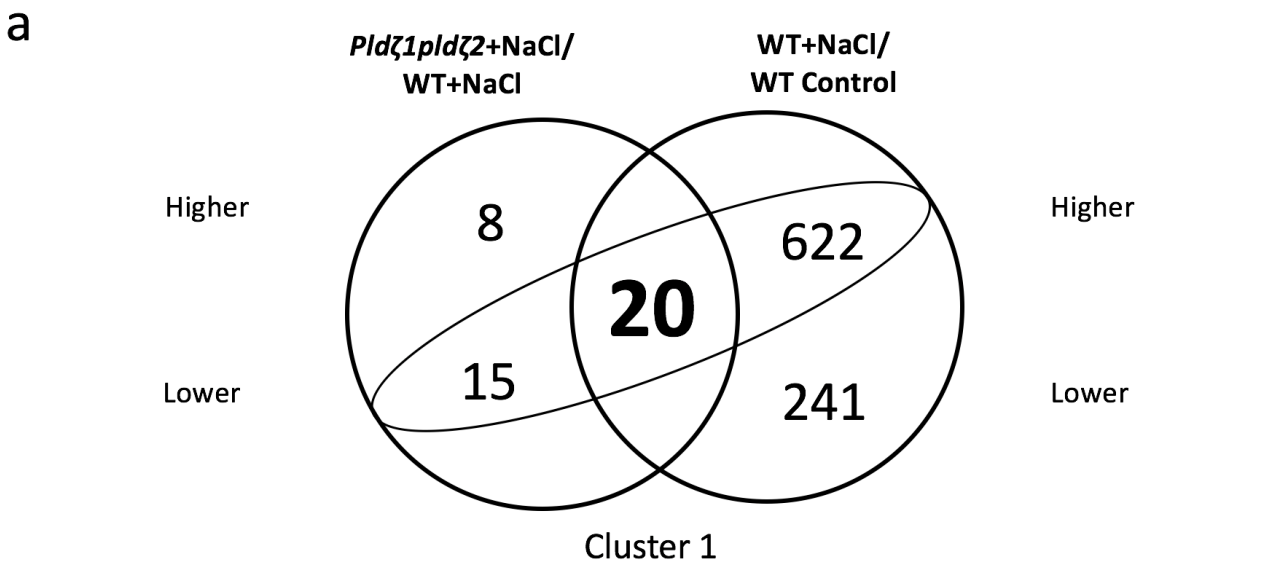

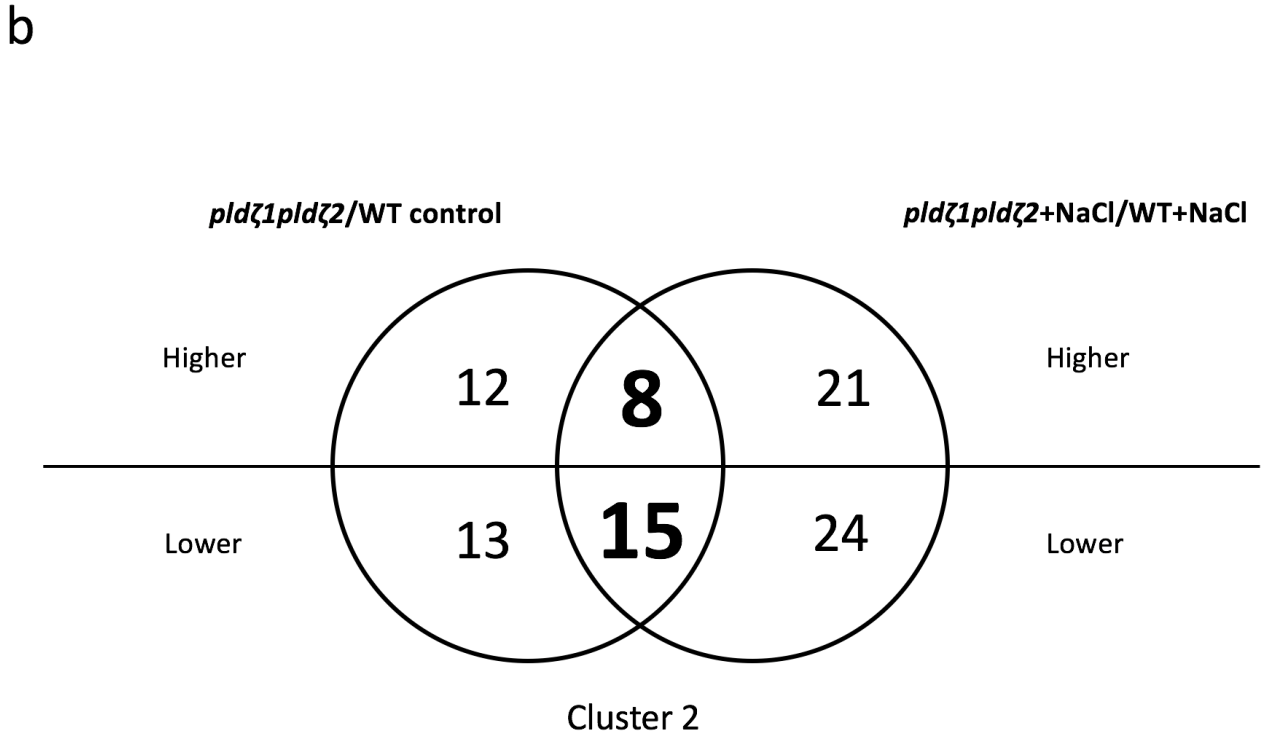

Figure 1. Numbers of differentially expressed genes in WT and *pldζ1pldζ2* transcriptome comparisons. Venn diagrams show how gene clusters were defined. (**a**) Cluster 1 (intersection in bold) includes genes which are induced by salt stress in WT and are expressed at lower levels in the double mutant under salt stress than in WT. (**b**) Cluster 2 (intersection in bold) includes genes which are up or down regulated in *pldζ1pldζ2* compared to WT in both control and salt stress conditions.

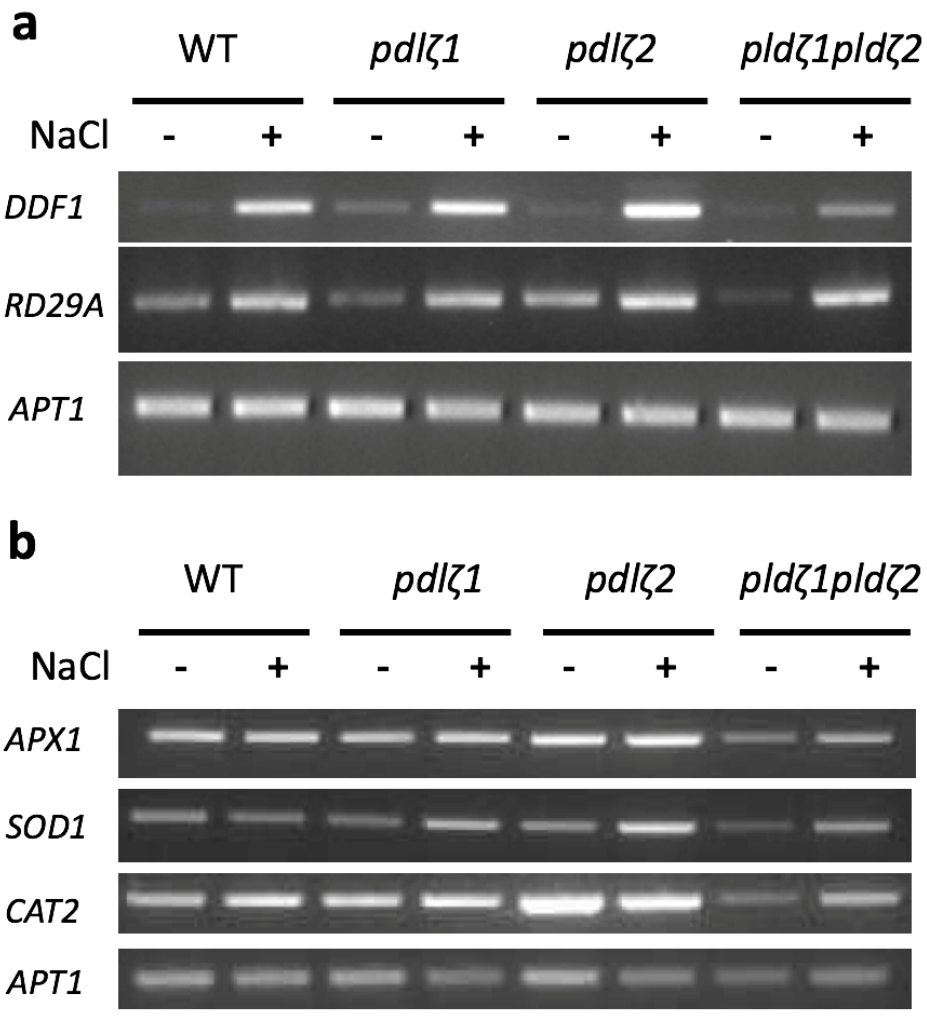
a
WT
pdlζ1
pdlζ2
pldζ1pldζ2
NaCl
- + - + - + - +
DDF1
RD29A
APT1
b
WT
pdlζ1
pdlζ2
pldζ1pldζ2
NaCl
- + - + - + - +
APX1
SOD1
CAT2
APT1
c
Relative DDF1 gene expression level
Relative RD29A gene expression level
0 2 4 6 8 10 12 14
NaCl
- + - + - + - +
WT
pdlζ1
pdlζ2
pldζ1pldζ2

666

Figure 2. Gene expression in wild-type (WT), *pldζ1*, *pldζ2* and *pldζ1ζ2* plants treated (+) or not treated (-) with 200 mM NaCl for 3 h. *DDF1* and *RD29A* (**a**), and *APX1*, *SOD1* and *CAT2* (**b**) expression was estimated by RT-PCR with *APT1* as a loading control. (**c**) Quantitative RT-PCR of *DDF1* and *RD29A* expression in WT, *pldζ1*, *pldζ2* and *pldζ1ζ2* seedlings. *DDF1* transcript abundance was expressed as a ratio of the value for WT in control conditions. *APT1* gene expression was used as a standard. Mean and standard errors are based on three technical repeats

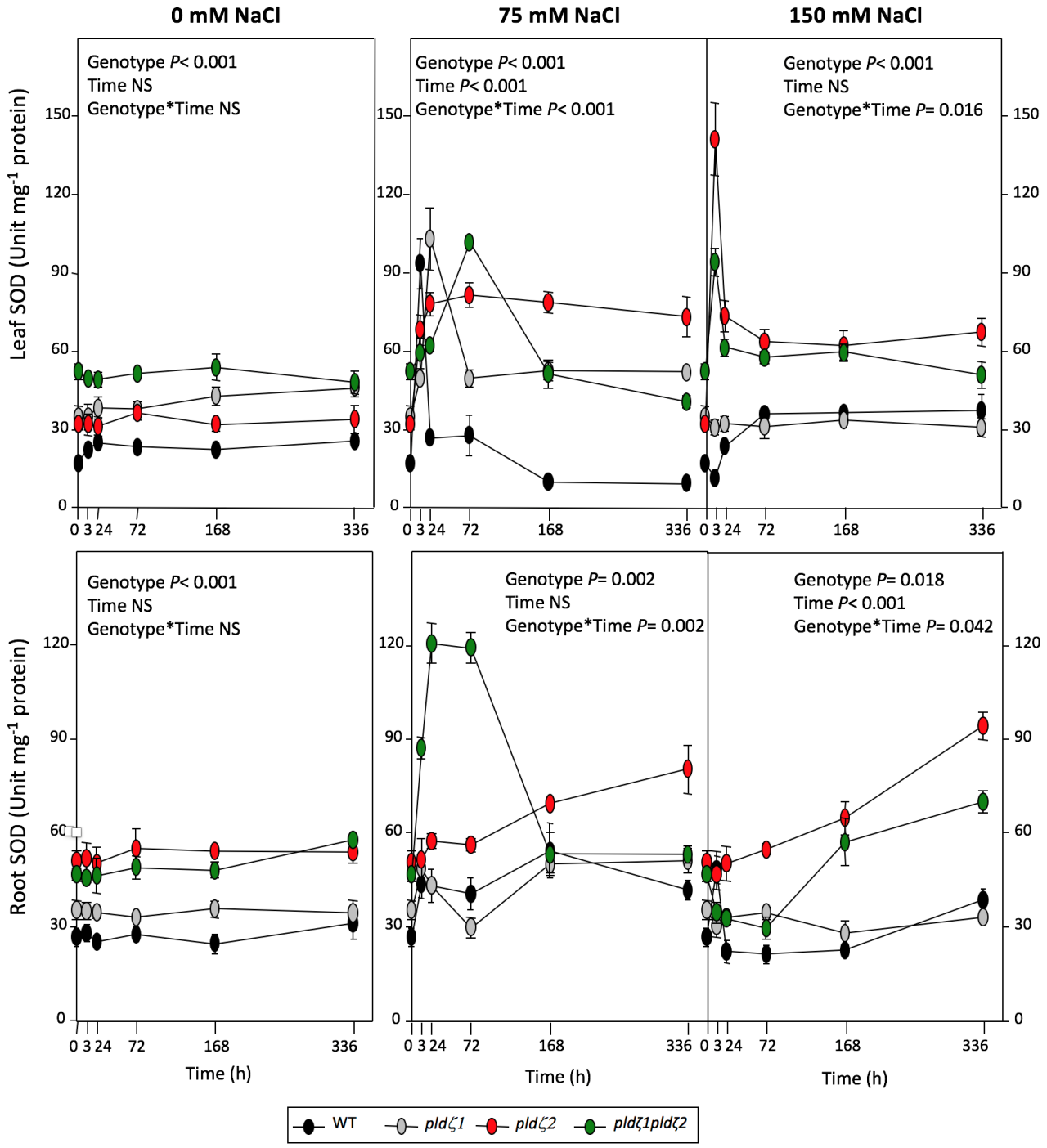

Figure 3. Changes in superoxide dismutase (SOD) activity in leaves and roots of wild type and *pldζ1*, *pldζ2* and *pldζ1pldζ2* mutants of *A. thaliana* plants grown for 14 days under moderate (75 mM NaCl) or severe salinity (150 mM NaCl). Data are means ± SE of 3 replicates. Results of statistical analysis are given in each panel (ANOVA, $P \leq 0.05$). NS, not significant.

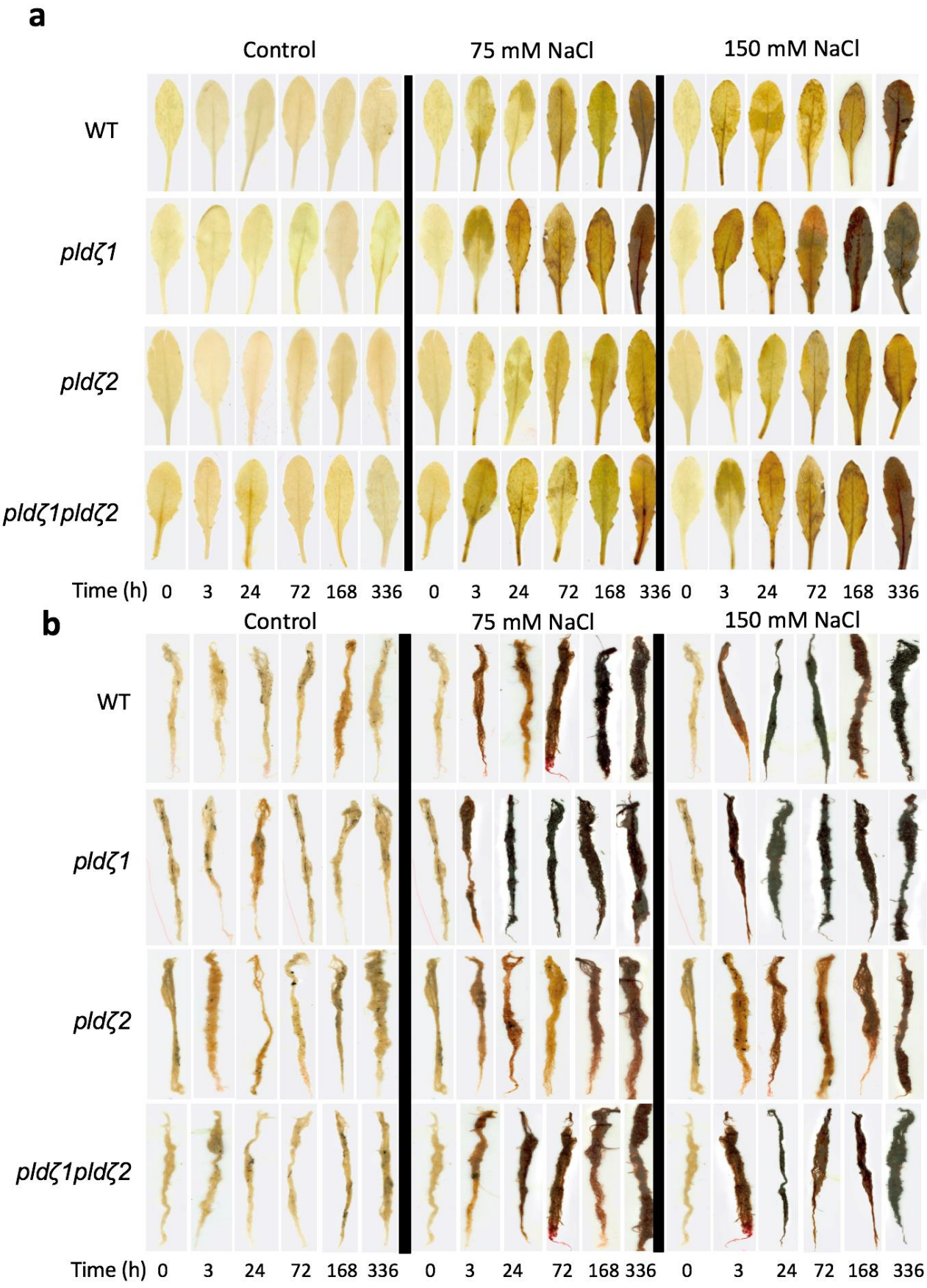
a
Control
75 mM NaCl
150 mM NaCl
WT
pldζ1
pldζ2
pldζ1pldζ2
Time (h) 0 3 24 72 168 336 0 3 24 72 168 336 0 3 24 72 168 336
b
Control
75 mM NaCl
150 mM NaCl
WT
pldζ1
pldζ2
pldζ1pldζ2
Time (h) 0 3 24 72 168 336 0 3 24 72 168 336 0 3 24 72 168 336

681

682 **Figure 4** Histochemical detection of hydrogen peroxide in leaves (a) and roots (b) of wild type and
683 *pldζ1*, *pldζ2* and *pldζ1pldζ2* mutants of *A. thaliana* plants grown for 14 days under moderate (75
684 mM NaCl) or severe salinity (150 mM NaCl). Brown residue from diaminobenzidine staining
685 indicates sites of H_2O_2 accumulation.
686

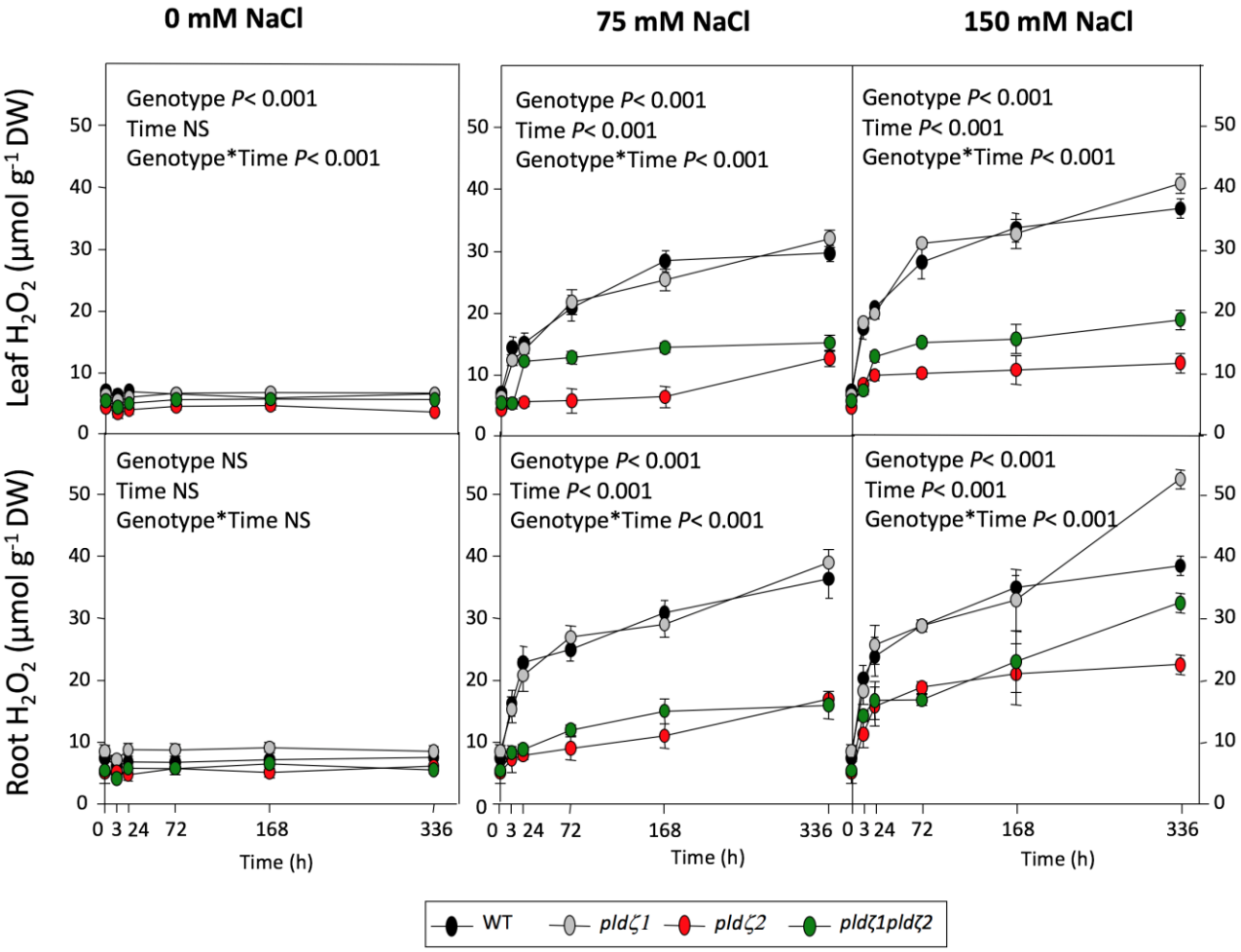

Figure 5. Changes in hydrogen peroxide levels in leaves and roots of wild type and *pldζ1*, *pldζ2* and *pldζ1pldζ2* mutants of *A. thaliana* plants grown for 14 days with moderate (75 mM NaCl) or severe salinity (150 mM NaCl). Data are means ± SE of 3 replicates. Results of statistical analysis are given in each panel (ANOVA, $P \leq 0.05$). NS, not significant.

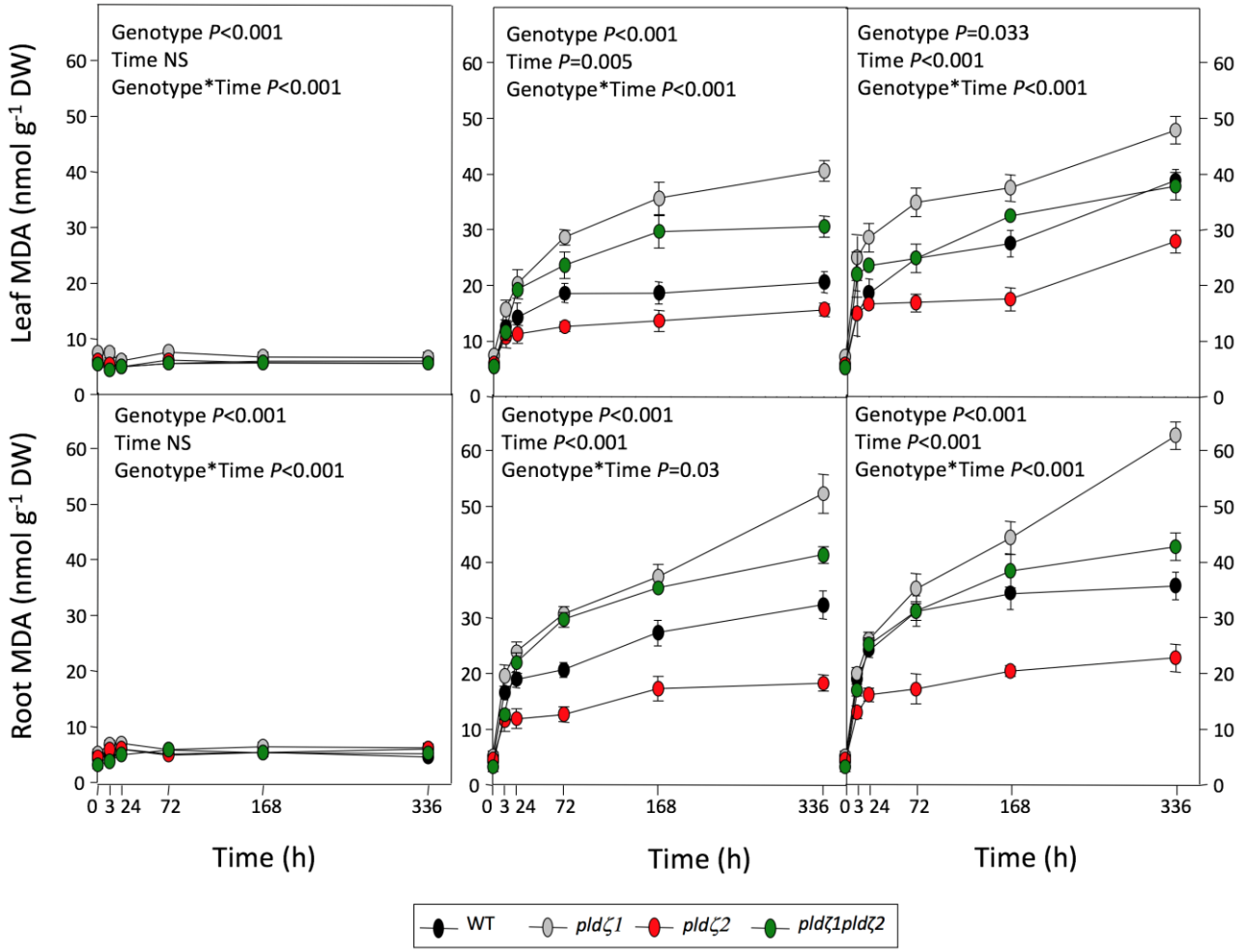

693

694 **Figure 6.** Changes in malondialdehyde (MDA) levels in leaves and roots of wild type and *pldζ1*,
695 *pldζ2* and *pldζ1pldζ2* mutants of *A. thaliana* plants grown for 14 days under moderate (75 mM
696 NaCl) or severe salinity (150 mM NaCl). Data are means ± SE of 3 replicates. Results of statistical
697 analysis are given in each panel (ANOVA, $P \leq 0.05$). NS, not significant.

698

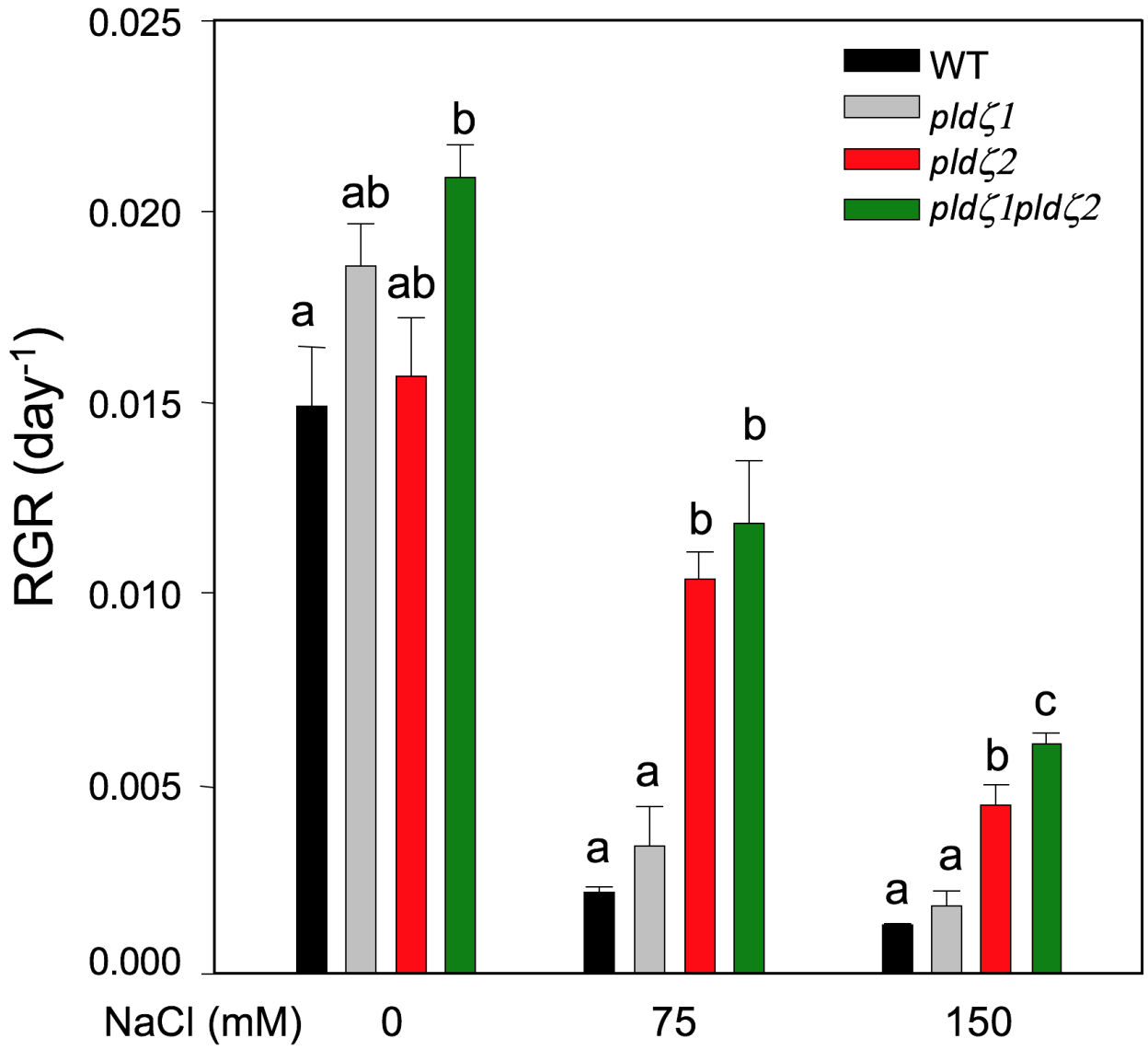

Figure 7. Relative growth rate (RGR) in *A. thaliana* single and double *pldζ* mutants grown for 14 days under control conditions or moderate (75 mM NaCl) or severe salinity (150 mM NaCl). Means indicated by different letters are significantly different ($P \leq 0.05$) as determined by one-way ANOVA.

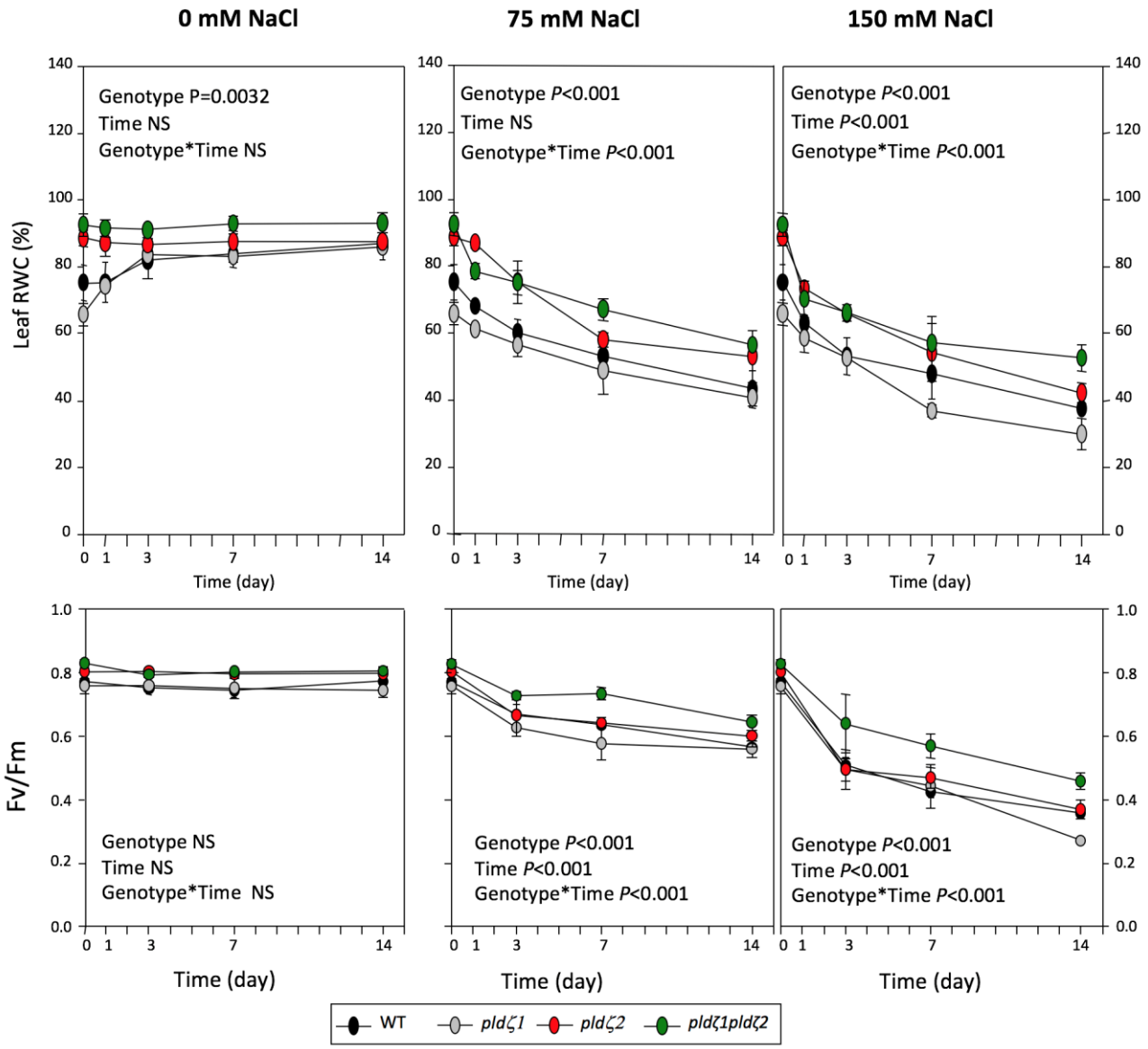

Figure 8. Changes in the relative water content (RWC) and in *Fv/Fm* ratios of leaves and roots of wild type, and *pldζ1*, *pldζ2* and *pldζ1pldζ2* mutants of *A. thaliana* plants grown for 14 days under moderate (75 mM NaCl) or severe salinity (150 mM NaCl). Data are means ± SE of 3 replicates. Results of statistical analysis (ANOVA, $P \leq 0.05$) are given in each panel. NS, not significant

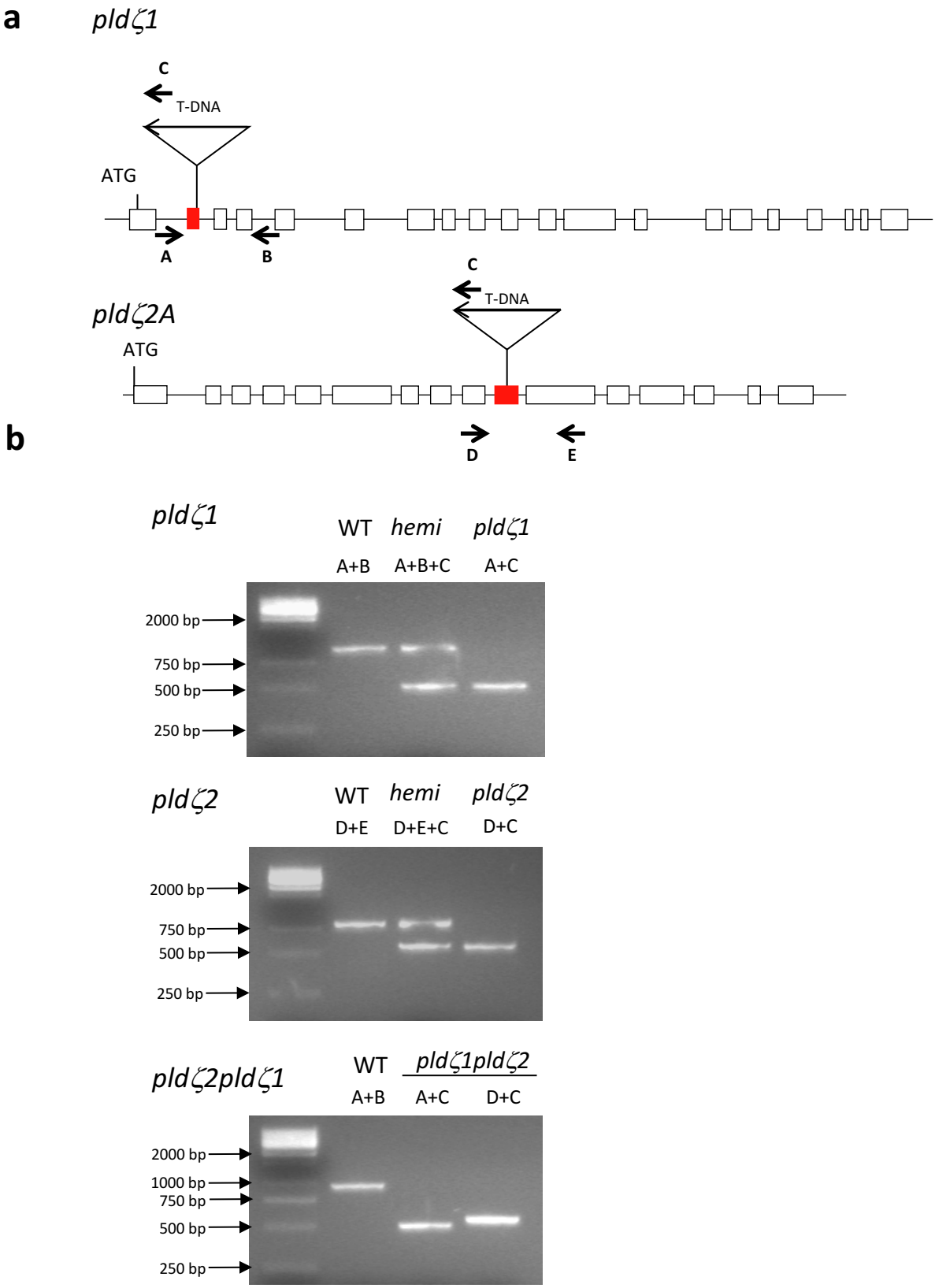

Supplementary Figure S1 Map and genotyping of *pldζ1*, *pldζ2* and *pldζ1pldζ2* mutants. (a) Map of T-DNA insertion site in *pldζ1* and *pldζ2* genes. Primers used for PCR are represented by arrows. (b) 1 % agarose gels of PCR products for *PLDζ1* WT allele (A+B), *pldζ1* T-DNA flanking sequence (A+C), or both (A+B+C) in hemizygous plants (top gel). PCR products for WT PLDζ2 WT allele (D+E), *pldζ2* T-DNA flanking sequence (D+C), or both (D+E+C) in hemizygous plants (middle gel). WT allele amplification (A+B), *pldζ1* T-DNA flanking sequence (A+C) and *pldζ2* T-DNA flanking sequence (D+C) in *pldζ1pldζ2 (*bottom gel).

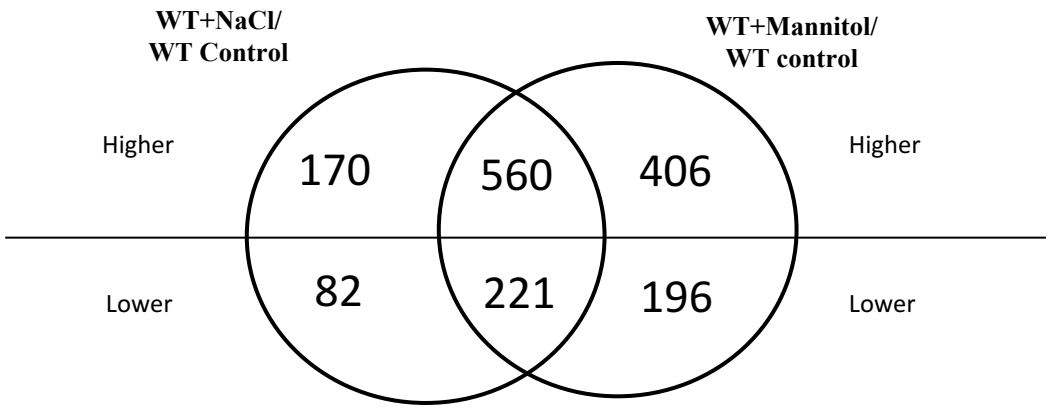

Supplementary Figure S2 Venn diagram of WT transcriptomes under salt and mannitol stresses in comparison to control growth conditions. Numbers of differentially expressed genes for each comparison are shown.

		WT+NaCl / WT control		pldζ1pldζ2+NaCl / WT+NaCl	
AGI	**Name**	*Log2 Ratio*	*Pvalue*	*Log2 Ratio*	*Pvalue*
AT1G12610	DDF1 transcription factor	**1.96**	0.00E+0	**-1.89**	0.00E+0
AT1G73480	alpha/beta hydrolase family	**3.40**	0.00E+0	**-1.04**	0.00E+0
AT5G52310	COR78 (COLD REGULATED 78) (RD29A)	**4.04**	0.00E+0	**-1.03**	5.60E-12
AT2G16500	ADC1_ arginine decarboxylase 1	**0.89**	1.17E-4	**-0.98**	1.12E-10
AT1G58360	AAP1; amino acid permease 1	**1.95**	0.00E+0	**-0.86**	1.77E-7
AT2G38240	oxidoreductase. 2OG-Fe(II) oxygenase	**1.23**	2.24E-11	**-0.81**	2.50E-6
AT5G13750	ZIFL1 zinc induced facilitator-like 1	**1.81**	0.00E+0	**-0.78**	9.68E-6
AT2G46370	JAR1 (JASMONATE RESISTANT 1)	**0.83**	1.15E-3	**-0.76**	2.66E-5
AT4G26080	ABI1 (ABA INSENSITIVE 1) PP2C family	**1.48**	0.00E+0	**-0.75**	4.51E-5
AT1G51090	metal ion binding	**2.99**	0.00E+0	**-0.74**	1.05E-4
AT1G72770	HAB1; PP2C homologue to ABI1	**2.53**	0.00E+0	**-0.73**	1.22E-4
AT3G07700	Protein kinase superfamily protein	**0.90**	8.80E-5	**-0.73**	1.57E-4
AT1G01650	SPPL4(SIGNAL PEPTIDE PEPTIDASE-LIKE 4)	**0.73**	4.31E-2	**-0.71**	3.41E-4
AT3G48990	AMP-dependent synthetase and ligase	**0.75**	2.14E-2	**-0.71**	3.61E-4
AT1G29400	AML5 (ARABIDOPSIS MEI2-LIKE PROTEIN 5)	**0.79**	5.23E-3	**-0.70**	5.50E-4
AT5G17760	P-loop nucleoside triphosphate hydrolase	**1.43**	0.00E+0	**-0.70**	6.32E-4
AT1G76960	unknown protein	**0.85**	7.24E-4	**-0.67**	2.25E-3
AT2G35940	EDA29 (BEL1-like homeodomain 1)	**0.80**	3.45E-3	**-0.65**	5.59E-3
AT4G15530	PPDK pyruvate orthophosphate dikinase	**0.90**	1.04E-4	**-0.64**	8.57E-3
AT5G55970	RING/U-box superfamily protein	**1.25**	5.59E-12	**-0.61**	2.51E-2

Supplementary Figure S3 List of genes in Cluster 1. Genes are involved in abiotic or biotic stimulus and response to stress. Expression data is given as $\log_2$ ratios.

Cluster 1 (Figure 1)	Normed to Freq. In Arabidopsis set (± bootstrap StdDev, p-value)		
Biological process	Frequence in Cluster 1	Std dev	P value
response to abiotic or biotic stimulus (Input set freq.: 0.65; 0.13)	4.96	0.795	0.00000009492
other biological processes (Input set freq.: 0.45; 0.12)	3.65	0.874	0.0002548
response to stress (Input set freq.: 0.5; 0.14)	3.45	0.681	0.0001537
developmental processes (Input set freq.: 0.4; 0.13)	3.02	0.91	0.002149
transport (Input set freq.: 0.35; 0.12)	2.82	0.814	0.006256
signal transduction (Input set freq.: 0.15; 0.07)	2.12	1.185	0.115

Cluster 2 (Figure 4)	Normed to Freq. In Arabidopsis set (± bootstrap StdDev, p-value)		
Biological process	Frequence in Cluster 2	Std dev	P value
electron transport or energy pathways (Input set freq.: 0.28; 0.02)	13.07	4.609	4.157e-06
response to stress (Input set freq.: 0.76; 0.13)	5.47	0.807	1.850e-10
response to abiotic or biotic stimulus (Input set freq.: 0.61; 0.13)	4.62	0.885	2.780e-07
other biological processes (Input set freq.: 0.57; 0.13)	4.28	0.815	2.565e-06
transport (Input set freq.: 0.38; 0.1)	3.57	1.227	7.785e-04
cell organization and biogenesis (Input set freq.: 0.33; 0.11)	2.81	0.94	6.493e-03
developmental processes (Input set freq.: 0.33; 0.12)	2.62	0.781	9.223e-03
signal transduction (Input set freq.: 0.14; 0.05)	2.53	1.084	0.083

http://bar.utoronto.ca/ntools/cgi-bin/ntools_classification_superviewer.cgi#annotation_list

Supplementary Figure S4 SuperViewer classification for genes listed in clusters 1 and 2.

		pldζ1ζ2 / WT control		*pldζ1ζ2*+NaCl / WT+NaCl	
AGI	**Name**	*Log2 Ratio*	*Pvalue*	*Log2 Ratio*	*Pvalue*
AT5G35935	unknown protein_ copia-like	**1.64**	0.00E+0	**1.73**	0.00E+0
AT1G23390	unknown protein	**1.28**	0.00E+0	**0.78**	1.40E-5
AT1G08830	CSD1; copper. zinc superoxide dismutase	**1.27**	0.00E+0	**0.78**	1.02E-5
AT1G66100	toxin receptor binding_ thionin. putative	**1.23**	0.00E+0	**0.65**	4.41E-3
AT1G12520	CCS1; superoxide dismutase copper chaperone	**1.04**	5.30E-9	**0.81**	2.04E-6
AT3G02380	COL2 transcription factor	**0.81**	3.05E-4	**0.64**	7.26E-3
AT5G48485	DIR1 lipid transfer protein (LTP)	**0.74**	3.99E-3	**0.60**	4.57E-2
AT4G09320	NDPK1 nucleoside diphosphate kinase type 1	**0.72**	7.93E-3	**0.73**	1.58E-4
AT3G48990	AMP-dependent synthetase and ligase	**-0.84**	7.33E-5	**-1.06**	0.00E+0
AT5G08530	CI5. NADH-ubiquinone oxidoreductase 51 kDa	**-0.85**	5.72E-5	**-0.95**	9.52E-10
AT3G23820	GAE6	**-0.87**	2.15E-5	**-1.09**	0.00E+0
AT5G05170	CESA3 (CELLULASE SYNTHASE 3)	**-0.92**	2.63E-6	**-0.98**	1.12E-10
AT4G32410	CESA1 (CELLULASE SYNTHASE 1)	**-0.94**	9.08E-7	**-1.00**	3.92E-11
AT3G46970	ATPHS2	**-1.01**	3.21E-8	**-1.09**	0.00E+0
AT1G59870	ABC transporter family protein	**-1.08**	8.23E-10	**-1.04**	0.00E+0
AT2G25490	EBF1 (EIN3-BINDING F BOX PROTEIN 1)	**-1.15**	1.12E-11	**-1.31**	0.00E+0
AT4G38770	PRP4 (PROLINE-RICH PROTEIN 4)	**-1.29**	0.00E+0	**-0.94**	1.15E-9
AT3G60750	transketolase_ transketolase. putative	**-1.31**	0.00E+0	**-1.01**	1.12E-11
AT3G33002	ribosomal protein S2p family	**-1.33**	0.00E+0	**-1.11**	0.00E+0
AT5G42020	ATP binding_ luminal binding protein 2 (BiP-2)	**-1.38**	0.00E+0	**-1.53**	0.00E+0
AT3G09440	HSP70-3	**-1.61**	0.00E+0	**-1.38**	0.00E+0
AT4G30650	low temperature and salt responsive protein	**-1.82**	0.00E+0	**-1.11**	0.00E+0
AT5G02500	HSC70-1	**-1.83**	0.00E+0	**-1.39**	0.00E+0

Supplementary Figure S5 List of genes in cluster 2. Genes are involved in electron transport, biotic and abiotic stress and stress responses. Expression data are given as $\log_2$ ratios.

Supplementary Table S1 List of primer sequences used for RT-PCR analysis and genotyping.

For RT-PCR

Gene name	Accession number	5'-3' Sequence
DDF1-F	AT1G12610	GGGACTTATCCCACAGCAGA
DDF1-R	AT1G12610	ATCATTGGATTCCGGCACC
RD29AF	AT5G52310	CAAAACAGAGCACTTACACAGAGAA
RD29AR	AT5G52310	CATAATCTCTACCCGACACACTTTT
APT1F	AT1G27450	GAGACATTTTGCGTGGGATT
APT1R	AT1G27450	CGGGGATTTTAAGTGGAACA
APX1F	X59600.1	CTGACATTCCTTTCCACCCT
APX1R	X59600.1	CAGACCTATCCTTGTGGCAT
CSD1F	AT1G08830	GGTTTCCATGTCCATGCTCT
CSD1R	AT1G08830	ATTGTGAAGGTGGCAGTTCC
CAT2F	AT4G35090.1	AACTCTGGTGCTCCTGTATGG
CAT2R	AT4G35090.1	CTCCAGTTCTCTTGGATGTG

For genotyping

A	PLDzeta1F	At3g16785	TCAGAATCACTTAAGAGGAGATGGG
B	PLDzeta1R	At3g16785	TTTTCGCATAGTCACTTGCTGT
C	LBb1	T-DNA left border	GCGTGGACCGCTTGCTGCAACT
D	PLDzeta2F	At3g05630	TCTCTGTTTTGGGCGGTACGA
E	PLDzeta2R	At3g05630	AAAATGTTCAGCGTTCTGGAT